Chem Soc Rev

Medical Micro/Nanorobots in Complex Media

Journal:	*Chemical Society Reviews*
Manuscript ID	CS-REV-03-2020-000309.R1
Article Type:	Review Article
Date Submitted by the Author:	13-May-2020
Complete List of Authors:	Wu, Zhiguang; California Institute of Technology Division of Engineering and Applied Science Chen, Ye; Santa Clara University, Department of Mechanical Engineering Mukasa, Daniel; California Institute of Technology Division of Engineering and Applied Science Pak, On Shun; Santa Clara University, Department of Mechanical Engineering Gao, Wei; California Institute of Technology Division of Engineering and Applied Science,

ARTICLE

Medical Micro/Nanorobots in Complex Media

Zhiguang Wu,[a] Ye Chen,[b] Daniel Mukasa,[a] On Shun Pak,[b] and Wei Gao*[a]

Received 31st March 2020,
Accepted 00th January 20xx

DOI: 10.1039/x0xx00000x

Medical micro/nanorobots have received tremendous attention over the past decades owing to their potential to be navigated into hard-to-reach tissues for a number of biomedical applications ranging from targeted drug/gene delivery, bio-isolation, detoxification, to nanosurgery. Despite the great promise, the majority of the past demonstrations are primarily under benchtop or *in vitro* conditions. Many developed micro/nanoscale propulsion mechanisms are based on the assumption of a homogeneous, Newtonian environment, while realistic biological environments are substantially more complex. Moving toward practical medical use, the field of micro/nanorobotics must overcome several major challenges including propulsion through complex media (such as blood, mucus, and vitreous) as well as deep tissue imaging and control *in vivo*. In this review article, we summarize the recent research efforts on investigating how various complexities in biological environments impact the propulsion of micro/nanoswimmers. We also highlight the emerging technological approaches to enhance the locomotion of micro/nanorobots in complex environments. The recent demonstrations of *in vivo* imaging, control and therapeutic medical applications of such micro/nanorobots are introduced. We envision that continuing materials and technological innovations through interdisciplinary collaborative efforts can bring us steps closer to the fantasy of "swallowing a surgeon".

1. Introduction

From "Fantastic Voyage" to "Swallowing a surgeon". In his inspiring talk in 1959, "There's Plenty of Room at the Bottom", Richard Feynman at the California Institute of Technology envisioned the era of small-scale machines. He described a fantasy by his student Albert Hibbs about swallowing a "micro-surgeon" streaming through blood vessels to perform micro-surgery. As funny as the idea sounded, we are now equipped with nanotechnology to realize the fantasy. This opens up new challenges on the design of these tiny machines. To date, miniaturization of robots to the micro/nanoscale attracts substantial attentions as they have the potential to be navigated into hard-to-reach tissues for a number of biomedical applications.[1-5] It should be noted that simply scaling down macroscopic machines would not work because various physical forces come out in different proportions when going down in size – "the rules of the game" at small scales are very different.

Challenges of swimming at small scales. For locomotion in fluids, inertial and viscous forces represent two major forces experienced by a swimmer. The relative importance of inertial to viscous forces is measured by the Reynolds number, $Re = \rho UL/\mu$, where U is a characteristic velocity, L is a characteristic length, and ρ *and* μ are density and dynamic viscosity of the fluid, respectively. Locomotion of larger animals (e.g., fishes and humans) in fluids occurs at moderate to large Reynolds numbers. In this regime, inertial forces dominate over the viscous forces. On the other hand, microorganisms and synthetic microswimmers inhabit a world of low Reynolds number. Taking the example of a microswimmer with a size $L \approx 10\ \mu$m and swimming speed $U \approx 10\ \mu$m/s in water, the Reynolds number is on the order of $Re \approx 10^{-4}$. The effect of inertia is thus virtually absent, rendering inertia-based propulsion mechanisms at the macroscopic scale largely ineffective in the world under the microscope.

The stringent constraints due to the absence of inertia are well illustrated by Purcell's scallop theorem.[6] As a result of kinematic reversibility, the scallop theorem rules out any reciprocal motion, the sequence of shape changes that has time-reversal symmetry, for self-propulsion at low Reynolds numbers. Hence, a "microscallop" opening and closing its shell periodically cannot swim in a Newtonian fluid regardless of the opening and closing rates. Rigid flapping motion is another type of reciprocal motion that is effective for propulsion at the macroscopic scale but ineffective in the microscopic world. Overall, the absence of inertia imposes a fundamental challenge on designing effective locomotion strategies at the microscopic scale (see a more detailed, pedagogical introduction on this subject).[7]

From swimming cells to synthetic swimmers. It is indeed a wonder when looking into the biological world, which has demonstrated to us diverse swimming strategies in the absence of inertia. Many microorganisms use one or multiple appendages, termed flagella and cilia, for swimming. These flagellated and ciliated microorganisms typically swim by propagating different types of flagellar waves to break the time-

[a] Andrew and Peggy Cherng Department of Medical Engineering, California Institute of Technology, Pasadena, CA, USA.
[b] Department of Mechanical Engineering, Santa Clara University, Santa Clara, CA, USA.
* Correspondence: weigao@caltech.edu.

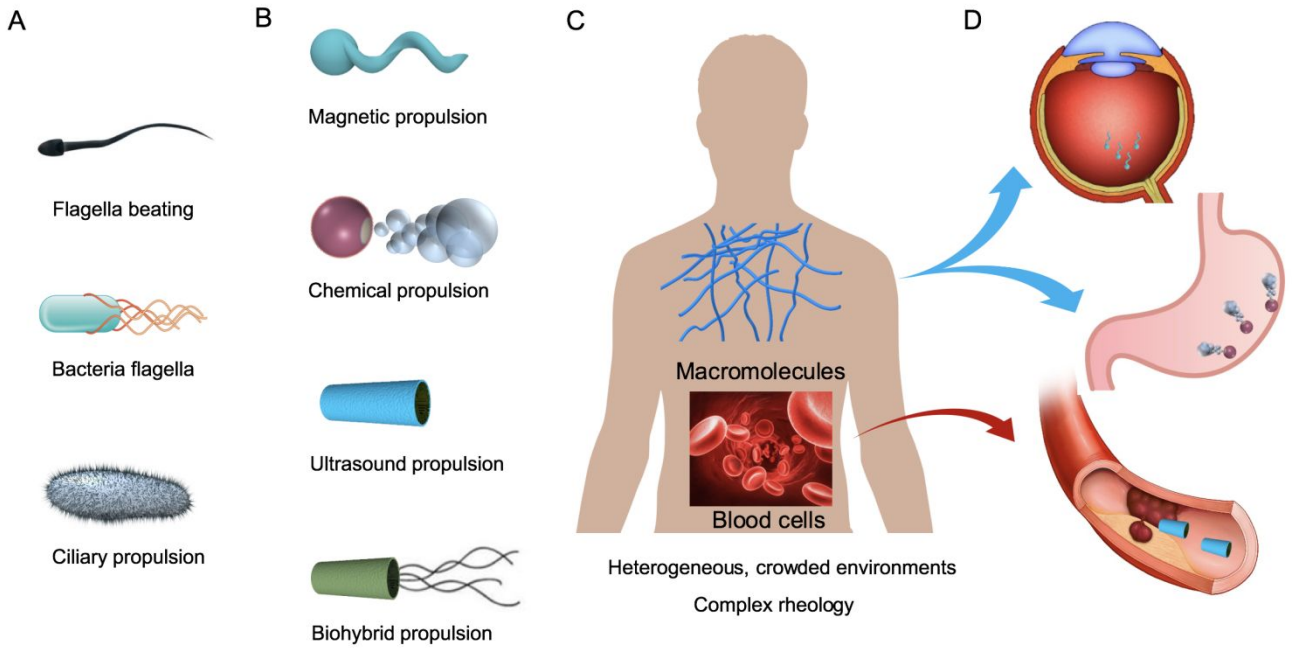

Figure 1. Medical micro/nanotobots in complex environments. (A) Major propulsion mechanisms of biological microswimmers, including flagellar beating for some eukaryotic cells, rotating helical bacterial flagella, and coordinated beating of cilia. (B) Major propulsion mechanisms of artificial microwimmers, including magnetic actuation of artificial flagella, chemical propulsion that relies on surrounding chemical fuels, ultrasound propulsion, as well as biohybrid propulsion. (C) In their biomedical applications, micro/nanorobots will invariably find themselves immersed in complex biological environments due to the presence of different biological macromolecules and cells. It is imperative to understand how heterogeneous, crowded environments and complex rheology impact their locomotion. (D) The emerging strategies employed to facilitate biomedical applications of micro/nanorobots in realistic biological environments such as microsurgery and drug delivery.

reversal symmetry. For instance, some spermatozoa beat their flexible flagella to propagate traveling deformation waves to swim in the opposite direction (**Fig. 1A**). Bacteria (e.g., *Escherichia coli)* swim by rotating their relatively rigid, helical flagella, which are connected to the rotary motor embedded in the cell body. Ciliates such as *Volvox* beat their arrays of cilia in coordinated manners to generate metachronal waves for swimming. Extensive theoretical and experimental studies in the past few decades illuminated the physical principles underlying cell motility,[8-12] which also resulted in different types of synthetic micro/nanoswimmers (**Fig. 1B**).[13-26]

Inspired by flagellar beating of microorganisms, flexible artificial microswimmers exploit the interaction between a flexible structure and its surrounding viscous fluid for propulsion. Dreyfus *et al.* developed a flexible magnetic filament consisting of colloidal magnetic particles connected by DNA.[27] Upon actuation by an external magnetic field, a beating pattern can be induced along the flexible magnetic filament to propel the structure. Flexible nanowire motors exploit similar elastohydrodynamic interaction to generate propulsion speeds comparable to natural microorganisms.[28-30]

Artificial helical swimmers represent a major class of swimmers that do not rely on swimmer's structural flexibility for propulsion. Instead, they mimic the relatively rigid and helical structure of bacterial flagella for propulsion. These chiral objects generate propulsive thrust due to the coupling of axial rotation with axial force, much like the corkscrew motion when opening a bottle of wine. While the rotation of bacterial flagella is due to the action of rotary motor embed in the cell body, artificial helical flagella are rotated by external magnetic fields.[31-33]

The flexible and helical swimmers introduced represent examples from the class of mechanical swimmers that rely on external fields (e.g., magnetic,[32, 34-39] electric,[40-42] acoustic,[43-49] light,[50-57] among others[58-60]) for actuation. Chemical swimmers, on the other hand, exploit chemical energy from their local environments for self-propulsion. These include self-phoretic Janus particles or nanowires that generate local solute concentration gradients (for self-diffusiophoresis) or local electrical potential gradients (for self-electrophoresis) due to asymmetries in surface activity.[5, 19, 61-73] In addition to phoretic locomotion, chemical reactions can generate bubbles to propel the particle by recoil forces. Since the propulsion mechanism is not phoretic, these bubble-propelled particles have more roust propulsion performance even in the presence of dissolved salts, an advantage over phoretic swimmers for biomedical applications.[74] Recent efforts have also taken a hybrid approach by combining multiple artificial propulsion mechanisms or integrating artificial and biological systems (biohybrid swimmers).[75-81] It should be noticed that in addition to the microswimmers, rolling and crawling-like surface surface-mediated locomotion have been utilized both in synthetic and

biohybrid microrobots.[82-87] All these propulsion strategies, together with other novel designs,[88-90] form a diverse spectrum of candidates for equipping biomedical micro/nanorobots with robust locomotive capabilities.

The tremendous efforts described above, however, only represent a first step towards turning the fantasy of "swallowing a surgeon" into reality. Recent studies have demonstrated the proof-of-concept applications of using these micro/nanoscale robots for targeted drug/gene delivery, bio-isolation, detoxification, and nanosurgery, primarily under benchtop or *in vitro* conditions (**Fig. 1C**).[18, 19, 90-92] Prior to achieving practical medical use, the field however must overcome a number of challenges including navigation through complex media as well as imaging and control under deep tissue *in vivo*.[90, 93] Many propulsion mechanisms are developed based on the assumption of a homogeneous, Newtonian environment, while realistic biological environments are substantially more complex (**Fig. 1C**). Here we define complex environments broadly as media that possess microstructures or heterogeneity across different length scales,[13, 14] which are typical of biological environments. The complexity of the media can manifest through non-Newtonian (nonlinear) rheological properties such as viscoelasticity and shear-thinning viscosity in biological fluids such as mucus and blood, due to the presence of suspended macromolecules or blood cells. Micro/nanoswimmers also need to navigate through crowded and heterogeneous environments, including the dense extracellular matrix (ECM) of biological tissues and barriers to invaders such as the blood-brain and gastric mucosal barriers, particularly for drug delivery applications. Propulsion mechanisms that are optimal in a certain medium may become largely ineffective in another. While biological cells can adapt their locomotion to effectively propel in complex fluids, navigate crowded environment, and invade biological barriers, it remains challenging to design micro/nanorobots with robust locomotive capabilities to perform similar tasks. Substantial interdisciplinary efforts have strived for a comprehensive understanding of how individual complexities and their combined presence in biological environments impact locomotion at small scales (see **Section 2**). In parallel, emerging techniques and engineering strategies have been proposed to facilitate the locomotion of micro/nanorobots in complex environments (see **Section 3**). These developments have led to recent demonstrations of *in vivo* imaging, control and therapeutic medical applications of such micro/nanorobots (**Fig. 1D**) (see **Section 4**). In this article, we review all three these avenues of research efforts and conclude on future directions that can bring us one step closer to "swallowing a surgeon".

2. Fluid dynamics of micro/nanoswimmers in complex environments

Synthetic swimmers that can move at the microscopic scale show great promise in biomedical applications, including drug delivery and microsurgery. In the past several decades, substantial progress has addressed the challenge of generating microscopic propulsion. Yet, successful applications of these swimmers to biomedical tasks rely on their ability to traverse realistic biological environments, which are much more complex than the homogeneous, Newtonian fluid media typically considered in theoretical models and experimental setups. Researchers have begun to examine the impacts of different complexities that can arise in more realistic biological systems, including heterogeneity in the environment (Section 2.1) and non-Newtonian rheological behaviors of biological fluids (Sections 2.2 & 2.3). Here we first introduce individual complex effects and review recent progress in developing a fundamental understanding of these effects, before discussing the engineering aspect of swimming in complex environments in subsequent sections. As a remark, although the focus on the current review is on synthetic swimmers, we also report studies involving biological organisms. These swimming organisms not only serve as model systems for understanding locomotion in complex environments but could also provide bio-inspired solutions for synthetic swimmers.

2.1 Interactions with boundaries and in crowded environments

In their natural habitats such as soil and the guts, biological organisms interact with different physical obstacles and boundaries, which may play essential roles in nature. For instance, interactions between bacteria and surfaces could induce attraction and adhesion of bacteria onto the surface in early stages of biofilm formation and pathogenic infection.[94-98] Sperm cells can navigate the female tract by a boundary-following guidance mechanism to reach the egg.[99, 100] The motility of blood parasites is adapted to swim in a crowded environment within the vertebrate bloodstream.[101] In their biomedical applications, synthetic micro/nanoswimmers will encounter the same complex biological environments. In this section, we discuss theoretical and experimental studies characterizing the interactions between swimmers and physical obstacles and boundaries.

Biological swimmers often find themselves immersed in heterogeneous environments with obstacles or fibers embedded into a viscous solvent (**Fig. 2A**).[102] The presence of these physical obstacles introduces additional no-slip and no-penetration surfaces, which alter the fluid flow around a swimmer and hence its locomotion performance. It is not obvious whether these interactions will enhance or hinder locomotion. The worm nematode Caenorhabditis elegans (*C. elegans*), which live in saturated soil, provide a model system to study locomotion in wet particulate systems (**Fig. 2B** and **2C**). Experiments observed that the propulsion speed of *C. elegans* is enhanced by the presence of particles.[103, 104] These experimental findings are consistent with theoretical predictions based on an effective medium approach for porous media,[104, 105] which captures the effect due to a sparse network of stationary obstacles as an averaged (mean field) equation, the Brinkman equation. Subsequent theoretical studies based on the Brinkman model with different types of swimmers further elucidate that swimming in porous media can be both enhanced or hindered, depending on details of the propulsion mechanism.[106-110] As a remark, the obstacles are assumed to be

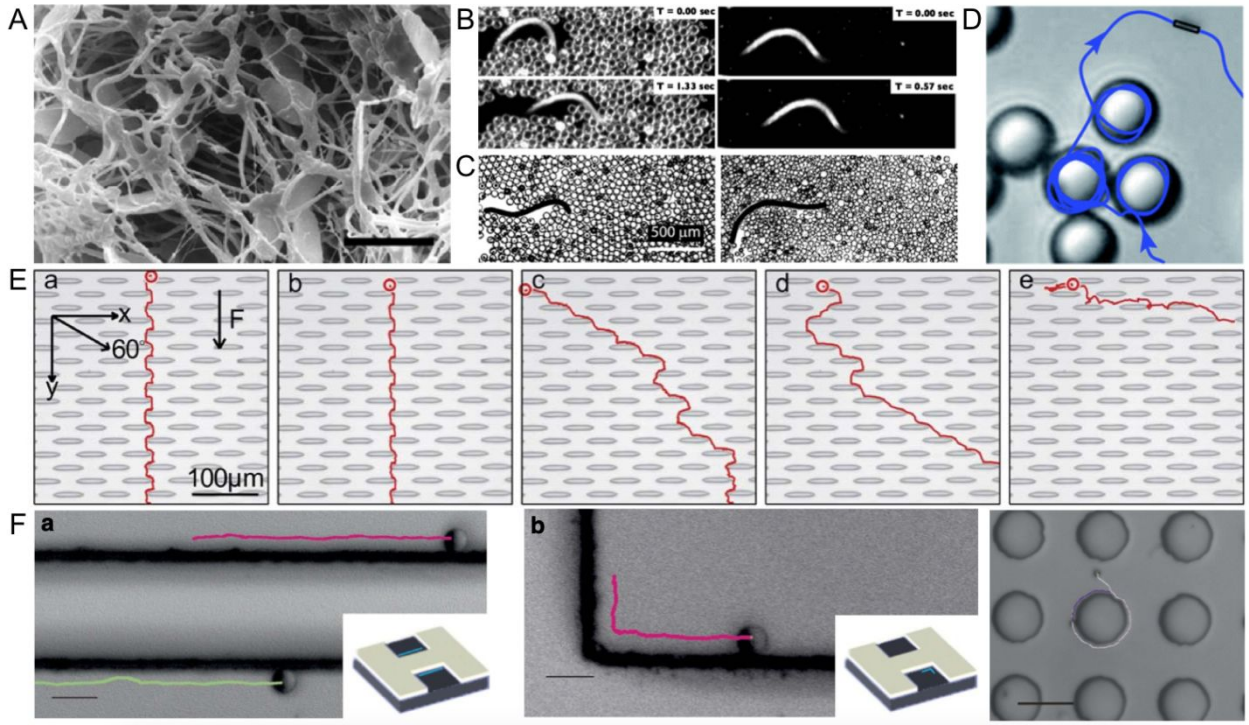

Figure 2. Locomotion in porous and crowded environments. (A) Photomicrograph of spermatozoa swimming in a vaginal fluid sample, a highly heterogeneous environment. Scale bar, 10 μm. Reproduced with permission from ref. 102. Copyright 2005 Wiley. (B) The nematode can swim faster in a wet particulate system (left) than in a homogeneous fluid (right). Reproduced with permission from ref. 104. Copyright 2010 AIP Publication. (C) Despite changes in motility behavior in wet monodisperse (left) and polydisperse (right) granular media, the stroke efficiency (the ratio of swimming speed to undulation speed) in wet granular media are higher than that in a fluid. Reproduced with permission from ref. 103. Copyright 2010 Europhysics Letters. (D) A phoretic microswimmer orbiting large colloids due to hydrodynamic interactions. Reproduced with permission from ref. 114. Copyright 2014 Royal Society of Chemistry. (E) Sorting of microswimmers in a pattern environment based on their swimming length, which is the average length of rather straight segments in the swimmer's trajectory. The swimming length increases from left (0, Brownian particle without self-propulsion) to right. Reproduced with permission from ref. 118. Copyright 2011 Royal Society of Chemistry. (F) Guidance of Janus particles by interactions with steps and obstacles: Janus particles following a straight step (left), maneuvering around a corner (middle), and moving around circular posts (right). Reproduced with permission from ref. 120. Copyright 2016 Nature Publishing Group.

stationary under the Brinkman medium approximation, and the deformability of the network can significantly impact swimming speeds.[111, 112]

When the network of obstacle is of the scale of the swimmer, the effect of the network on locomotion may not be captured using an effective medium approach. Local interactions between the swimmer and the surface of its neighboring obstacle become dominant. In addition to modifying the swimming speed, the surface can also re-orient a swimmer,[10, 13, 113] leading to scattering or entrapment of the swimmer around obstacles. Recent experiments show that bacteria and synthetic microswimmers can escape or be trapped around convex surfaces of micropillars or colloids.[114-117] For instance, a microswimmer approaching a small colloid can be simply scattered, while the swimmer can also orbit a sufficiently large colloid, as observed in experiments with phoretic swimmers (**Fig. 2D**).[10] With appropriate topographical designs, these hydrodynamic interactions can be exploited for sorting (**Fig. 2E**)[118, 119] and guiding (**Fig. 2F**)[120, 121] of microswimmers.

As a remark, in addition to hydrodynamic effects, recent studies have also highlighted the importance of steric effects in swimmer-wall interactions, especially for flagellated and ciliated swimmers.[122-125] Overall, over longer time scales, the fluctuations in swimming speed, scattering and trapping dynamics can all act together to affect the transport and dispersion of active particles in porous and crowded environments, which is another area of research with considerable recent attention.[126-132]

2.2 Complex rheology – viscoelasticity

Due to the presence of suspending microstructures formed by different kinds of macromolecules, many biological fluids are viscoelastic, meaning that the fluids have both viscous and elastic properties. Unlike a simple Newtonian fluid, a viscoelastic fluid possesses a memory of the flow history. The presence of elastic stress in viscoelastic fluids leads to interesting phenomena such as the rod-climbing effect (or the

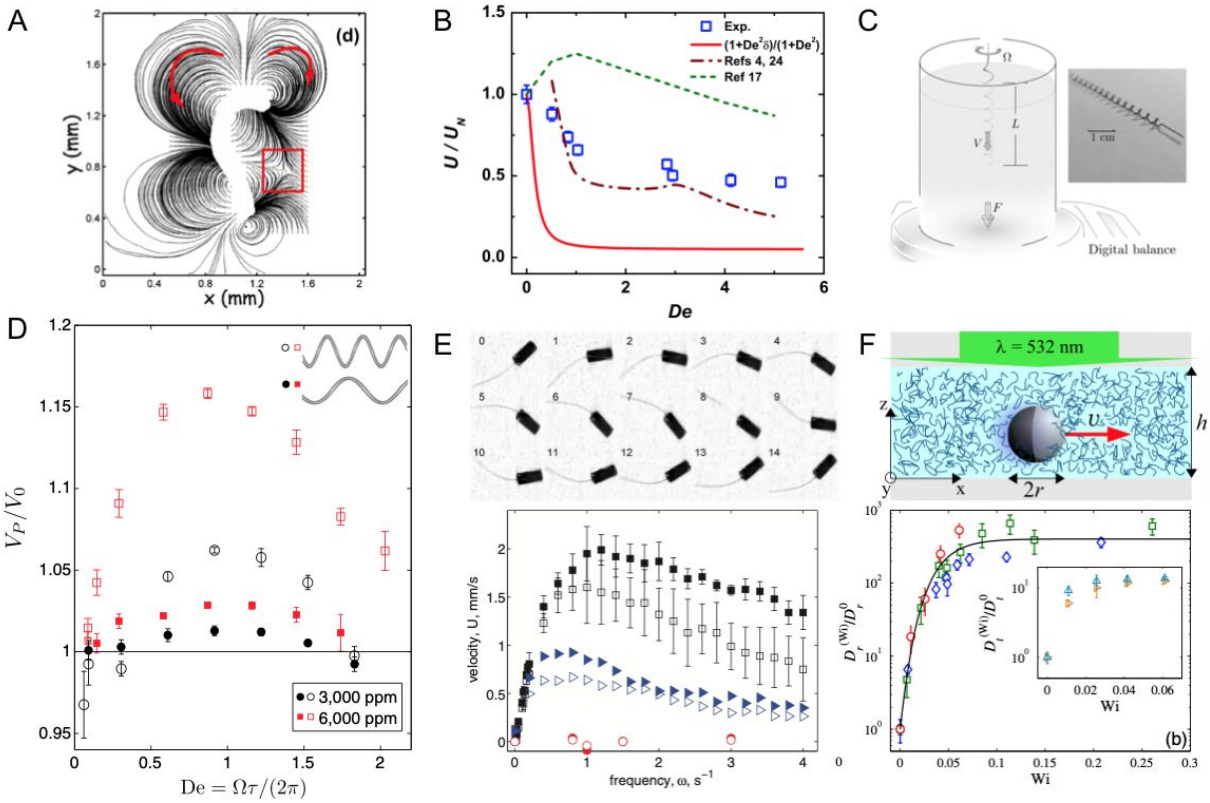

Figure 3. Locomotion in viscoelastic fluids. (A) Streamlines around the nematode *C. elegans* swimming in a viscoelastic fluid. The red box shows a hyperbolic point in flow, which was suggested to be related to the decrease in propulsion speed U relative to its Newtonian value U_N. Reproduced with permission from ref. 137. Copyright 2011 American Physical Society. (B) due to stretching of flexible molecules and hence increase of elastic stresses near the hyperbolic point. The Deborah number, $De = \lambda f$, compares the fluid relaxation time λ to the time scale of the beating motion (the inverse of the beating frequency, $1/f$). Reproduced with permission from ref. 137. Copyright 2011 American Physical Society. (C) Experiments of force-free swimming of a model helical flagellum rotating in viscoelastic fluids showed enhancement swimming around $De = 1$ (D). We note that a highly viscous fluid was employed in the macroscopic setup (at the centimetre scale) to maintain a low Reynolds number environment, ensuring dynamic similarity to locomotion at the microscopic scale. Reproduced with permission from ref. 139. Copyright 2011 National Academy of Sciences USA. (E) A magnetically actuated flexible swimmer displays systematically increased propulsion speeds in different viscoelastic fluids (filled symbols) compared with the corresponding Newtonian fluid (empty symbols). The red filled and empty circles represent results for rigid swimmers. Reproduced with permission from ref. 141. Copyright 2013 AIP Publication. (F) A Janus colloidal particle in viscoelastic fluid showed substantially enhanced rotational diffusion coefficient relative to its Newtonian value as a function of the Weissenberg number, Wi. Inset: the translational diffusion coefficient was also enhanced but to a less extent. Reproduced with permission from ref. 161. Copyright 2016 American Physical Society.

Weissenberg effect), die swell (or the Barus effect), among others.[133] The central question of whether fluid elasticity enhances or hinders locomotion has received substantial attention in the past several decades.[134, 135]

Theoretical calculations showed that the swimming speed of a small-amplitude waving sheet[133] and cylinder[136] both decrease in a viscoelastic fluid. Consistent with these predictions, experiments with *C. elegans* in viscoelastic fluids (carboxy-methyl cellulose solutions) measured 35% slower propulsion (Fig. 3A and 3B).[137] On the other hand, numerical simulations with a finite-length waving sheet model showed that fluid elasticity can increase the speed of a swimmer with large and increasing amplitude of undulations along the sheet.[138] Subsequent experiments and numerical simulations with model helical propellers also showed that fluid elasticity can either increase or decrease the swimming speed (Fig. 3C and 3D), depending on geometrical details of the helical propeller, its rotating rate, and properties of the surrounding fluid.[139, 140] These factors affect the distribution of polymeric stresses around the swimmer, which could contribute to the observed enhancement or hindrance of locomotion. We remark that swimming gaits of these undulatory and helical swimmers are prescribed. For a flexible swimmer, whose gaits are not known a *priori* but emerge as a result of fluid-structure interaction, the physical picture becomes even more complex. Experiments on a flexible swimmer, which consists of a magnetic head (actuated in rotation magnetically) and a flexible tail, measured systematically increased propulsion speeds in viscoelastic fluids compared with the speeds in Newtonian fluids (Fig. 3E).[141] Recent theoretical and numerical studies have

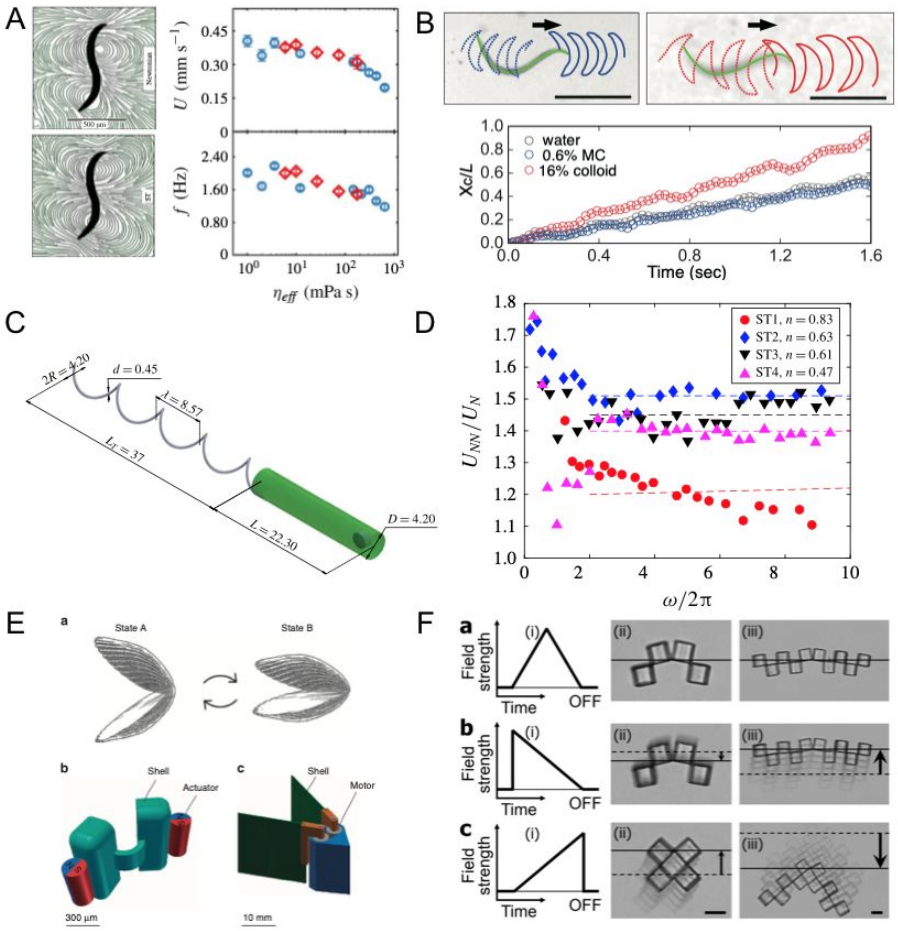

Figure 4. Locomotion in shear-thinning fluids. (A) The nematode *C. elegans* displayed similar locomotion performance in shear-thinning xanthan gum solutions (red symbols) as in Newtonian fluids (blue symbols). Reproduced with permission from ref. 174. Copyright 2014 Cambridge University Press. (B) On the other hand, experiments on *C. elegans* in colloidal suspensions, which display shear-thinning rheology, observed enhanced swimming. Reproduced with permission from ref. 176. Copyright 2016 Royal Society of Chemistry. (C) A magnetically actuated helical swimmer also displayed up to 50% faster propulsion speeds than the corresponding Newtonian cases (D). Reproduced with permission from ref. 177. Copyright 2016 Cambridge University Press. (E) Shear-thinning rheology was exploited to enable locomotion by the reciprocal motion due to the opening and closing of a single-hinge scallop. Reproduced with permission from ref. 181. Copyright 2014 Nature Publishing Group. (F) The swimming direction of microscallops formed by an assembly of microcubes in shear-thinning fluids can be adjusted by length of their arms. Reproduced with permission from ref. 182. Copyright 2020 American Chemistry Society.

shed light on how the gait, fluid elasticity, and body flexibility can interact in intricate manners to slow down or speed up a flexible swimmer.[142-146] In another avenue of research, researchers have considered simple mechanisms to exploit fluid elasticity to enable locomotion otherwise impossible in a Newtonian fluid, including rigid flapping motion,[147, 148] rotating,[149] spinning, [150] and oscillating[151] dumbbells, highlighting the role of fluid elasticity.

The squirmer model was first proposed by Lighthill and Blake for ciliary propulsion,[152, 153] represents an active particle with prescribed surface velocities. It has become a popular, generic swimmer model for locomotion in viscoelastic fluids,[154-158] because various types of swimmers (e.g., pushers versus pullers) can be represented by tuning the distribution of surface velocities on the squirmer.[10, 159] More recently, this framework has been coupled to the transport of solutes to investigate the dynamics of self-phoretic Janus particles in weakly viscoelastic fluids at low and finite Peclet numbers.[15, 160] These Janus particles were found to swim either slower or faster in the viscoelastic fluid relative to a Newtonian fluid depending on the distribution of surface activity.

In addition to propulsion speed, the effects of the viscoelastic response of fluid on the translational and rotational diffusion of Janus colloidal particles have been studied in a recent experiment.[161] While both translational and rotational diffusion was found to be enhanced in a viscoelastic fluid, the enhancement in rotational diffusion was particularly pronounced (up to 2 orders of magnitude) (**Fig. 3F**). Mesoscale simulations of an active colloid in a polymeric solution observed similar drastic enhancement of rotational diffusion.[162] The simulations suggested that the enhancement is due to the combined effects of a reduced amount of polymer adsorption by activity and an asymmetric encounter of the active particle with polymers. Mesoscale modeling of polymeric solutions

represents a different route than the use of non-Newtonian rheological constitutive models in studying locomotion in complex fluids.[163] Recent mesoscale simulations of bacterial swimming in polymeric solutions provide the resolution to capture the non-uniform polymer densities around the bacterium,[164] showing the role of polymer depletion around the swimmer in enhancing its swimming speed.[165-167]

Extensive theoretical and computational studies so far have generated valuable physical insights on different aspects of locomotion in biological fluids. Yet, a comprehensive physical picture across different length scales and types of swimmers remains to be formed. This requires closer connections between predictions from different theories and simulations and experimental measurements.

As a remark, complex fluids often display other non-Newtonian rheological behaviors in addition to viscoelasticity, such as shear-thinning viscosity (see Section 2.3). To isolate the effect of viscoelasticity on locomotion, viscoelastic constitutive models with constant viscosity (e.g., the second-order fluid model, the Oldroyd-B model, among others[133]) are used in theoretical and computational studies. Similarly, experimental studies typically employed complex fluids that behave approximately as a Boger fluid, a viscoelastic fluid with constant viscosity. This enables a fundamental understanding of the impacts due to individual complex rheological behaviors before examining their combined effects.

2.3 Complex rheology-shear-thinning rheology

In addition to viscoelasticity, another ubiquitous non-Newtonian behavior of biological fluids is shear-thinning: the fluid loses viscosity with increased shear rates as a result of changes in the fluid microstructure. Shear-thinning viscosity can lead to some encounter intuitive phenomena such as the Kaye effect[168] (or the "leaping shampoo" effect[169]). Compared with viscoelasticity, the effect of shear-thinning rheology on locomotion is much less studied. Yet, it is estimated that the shear-thinning effect could be several orders of magnitude more influential than viscoelasticity based on a waving sheet model.[170]

One may expect the shear-thinning effect to enhance self-propulsion because of the reduced viscosity and hence lower viscous drag on the swimmer. Yet, the shear-thinning effect not only decreases the viscous drag but could also simultaneously the propulsive thrust. Theoretical and computational studies on a variety of swimmers in shear-thinning fluids have revealed cases where the swimming speed can increase, decrease, or remain change compared with the Newtonian speeds. For undulatory swimmers, while an asymptotic analysis on the swimming of small-amplitude waving sheet suggested that the swimming speed is unaffected by the shear-thinning rheology,[170] numerical simulations showed that enhanced swimming is possible for swimmers with larger amplitudes.[171-173] Experiments on *C. elegans* in xanthan gum solutions (**Fig. 4A**)[174, 175] and colloidal suspensions (**Fig. 4B**),[176] which both display shear-thinning viscosities, measured equal or greater swimming speed, respectively. On the other hand, experiments on a magnetically actuated helical propeller in various shear-thinning, inelastic fluids measured up to 50% faster propulsion speeds than the Newtonian case (**Fig. 4C** and **4D**).[177] As a remark, one should use caution when extending the Newtonian concept of drag and thrust decomposition to non-Newtonian swimming due to the inherent nonlinearity of the problem, which can be significant enough to yield flawed predictions as illustrated via a squirmer model.[178]

Active efforts have begun to illuminate the physical mechanisms underlying these different observations on locomotion in shear-thinning fluids. When a fluid is no longer Newtonian but shear-thinning, the effect can manifest through both a local effect where the local shear stress reduces as a result of local viscosity reduction, and a non-local effect due to modifications of the fluid flow around the swimmer. [177, 179] An empirical model showed how the first local viscosity reduction effect can hinder swimming for slender bodies.[179] On the other hand, the observed enhanced locomotion for undulatory and helical swimmers may be attributed to the non-local effect. These swimmers often themselves in low-viscosity regions embedded in high-viscosity domains, resulting in a soft confinement that could lead to enhanced propulsion.[167, 173] The relative contributions of these local and non-local effects remain to be examined for swimmers with different geometries and propulsion mechanisms.[180]

Similar to the idea of exploiting fluid elasticity to enable locomotion (see **Section 2.2**),[147-150] researchers have also exploited shear-thinning rheology to render some reciprocal motion, incapable of generating self-propulsion in Newtonian fluids, effective for locomotion. Specifically, the swimming of single-hinged scallops is enabled in shear-thinning fluids by adjusting the rates of opening and close their hinges to take advantage of the shear-rate-dependent viscosity (**Fig. 4E**).[181] A recent study has further decreased of the size of these scallops to the microscopic scale by an assembly of patchy microcubes (**Fig. 4F**),[182] whose swimming direction can be adjusted by varying the geometric length of their arms.

2.4 Concluding remarks

The above sections showcase how various complexities present in biological environments impact the propulsion performance of micro/nanoswimmers, under different controlled experimental conditions or simplifying assumptions in theoretical and computational studies. Further studies are needed to fully elucidate the physical mechanisms underlying the changes and the combined presence of different complex factors. Nevertheless, we summarize below some possible implications of the above findings on the design of micro/nanoswimmers in complex media.

In porous media, the presence of sparse network of obstacles has been predicted to consistently enhance the propulsion of helical propellers. For flexible swimmers, it is plausible to adjust the size (relative to the pore size) and stiffness of the propeller to maximize the speed enhancement. Practical design guidelines and experimental characterization however are still lacking, which requires future considerations. For propulsion in viscoelastic fluids, enhanced propulsion could be achieved by tuning the actuation frequency of helical and

flexible propellers to match the relaxation time of a viscoelastic fluid, for a Deborah number on the order of 1 to 10. For self-phoretic particles, both translational and rotational (more substantial) diffusion increased with the Weissenberg number. Furthermore, recent theory suggested that breaking the fore-aft asymmetry of the two halves of a Janus particle can lead to increased swimming speed in a viscoelastic fluid, which calls for experimental implementation and characterization. Finally, the effect of the other type of non-Newtonian rheology, shear-thinning viscosity, appears to be the most pronounced when the actuation time scale of the swimmer is comparable with the time constant of the shear-thinning fluid, i.e., Carreau number on the order of 1 to 10. While some simulation suggested that some undulatory swimmers could swim faster in a shear-thinning fluid, theory suggested that self-phoretic Janus particle would swim slower, even with different adjustment fore-aft asymmetry in the small Peclet number limit; the effect of advection remains not fully characterized. Experiments on helical propellers showed consistently enhanced swimming speed in a shear-thinning fluid upon different actuation frequency, with the most pronounced enhancement occurring in fluid power index around 0.6.

We also remark that biological fluids are typically both shear-thinning and viscoelastic. Previous studies have revealed that shear-thinning rheology and viscoelasticity together can amplify phenomena otherwise not observed in Newtonian fluids (e.g., chaining of spheres[183-185] and titling of slender bodies during sedimentation[184, 186]). However, there is a gap of knowledge on the complex interactions of these non-Newtonian behaviors and their relative importance to locomotion at the microscopic scale. To unravel these effects and quantity their contributions and interactions would require the use of complex fluids with distinct non-Newtonian rheology in experiments[186, 187] and a variety of rheological constitutive models for comparison.[173, 188] Efforts along these directions have begun but are only limited to a few types of swimmers.[173, 187] The physical picture could vary substantially across swimmers with different physical and physico-chemical propulsion mechanisms.

Finally, there are other kinds of complexities, such as the presence of different physiological flows, dissolved salts, and environmental noises that could significantly affect the propulsion performance of different micro/nanoswimmers. While a detailed review of these factors is beyond the current scope, some of them will be briefly discussed in the following sections as they arise.

3. Synthetic micro/nanorobots in complex environments

Studies in Section 2 focus on model swimmers in complex yet idealized environments. In parallel, efforts with actual synthetic micro/nanorobots in realistic complex environments have revealed various practical challenges and potential solutions to facilitate their operations. We first examine the performance of existing propulsion mechanisms in biological fluids in **Section 3.1**, and then discussing strategies to enhance the performance of these micro/nanorobots in complex media (blood and biological porous media) in **Sections 3.2** and **3.3**.

3.1 Synthetic swimmers in biofluids

The past decades have seen the development of a significant number of micro/nanoswimmers based on chemical, physical, and biohybrid mechanisms (see **Section 1**). Their propulsion performance has been evaluated in different biological environments (such as human serum, cell culture, and gastrointestinal fluids), an important step toward propulsion in complex media. For some chemical swimmers, such as self-diffusiophoretic and self-electrophoretic particles, their performance is dramatically impaired in biological fluids due to the presence of proteins and electrolytes.[22, 68, 189, 190] In comparison, certain bubble-based mechanisms (utilizing biofluids as the fuel instead of classic H_2O_2 fuel) yield considerable performance for the propulsion of micro/nanorobots in various biofluids.[19, 61, 63, 191] For example, magnesium-based Janus microrobots exhibit efficient propulsion in cell media via the thrust of hydrogen bubbles produced by the reaction of magnesium with water.[192-195] Bubble propelled magnesium-based Janus microrobots modified with macrophage cells have been demonstrated in the GI tract and display high-speed propulsion enabling enhanced tissue penetration, retention of macrophage biological functionality, and thus enhanced therapeutic efficiency (**Fig. 5A**).[196] Recently Nitric Oxide (NO)-driven nanorobots, constructed by the assembly of hyperbranched polyamide and L-arginine and powered by the conversion of L-arginine to NO with NO synthase or reactive oxygen species, have been reported in cell media as well.[197]

For synthetic swimmers relying on actuation by external fields, magnetic flexible nanowire motors demonstrated robust propulsion performance in untreated human serum samples; [28] yet, the effects due to the presence of blood cells were not accounted for. Helical micro/nanostructures (**Fig. 5B**) [31, 33, 198-201] can be driven by rotating magnetic fields to pass through hyaluronan solution, a polymeric viscoelastic gel appearing in different biological tissues (see **Section 3.3** for more details).[194] In addition, acoustically powered bubble-based microswimmers were developed that could be used for transporting cells (**Fig. 5C**).[202] Compared with previously reported microswimmers, which rely on the pressure nodes in the acoustic field,[44, 203] these acoustic bubble-propelled microrobots endow efficient propulsion in cell culture media with the help of secondary Bjerknes forces and local acoustic streaming propulsive forces.[202]

In addition, bacteria and spermatozoa can be exploited as means of propulsion as well by loading them, either physically or chemically, with therapeutic cargo in the form of various microstructures.[204, 205] These bio-hybrid approaches harness biological swimmers' naturally evolved ability to traverse complex environments. Both *E. coli* and erythrocyte-hybrid microrobots have been fabricated with chemical biotin-streptavidin-biotin binding for such application. Erythrocyte loaded with magnetic materials and therapeutic agents can be

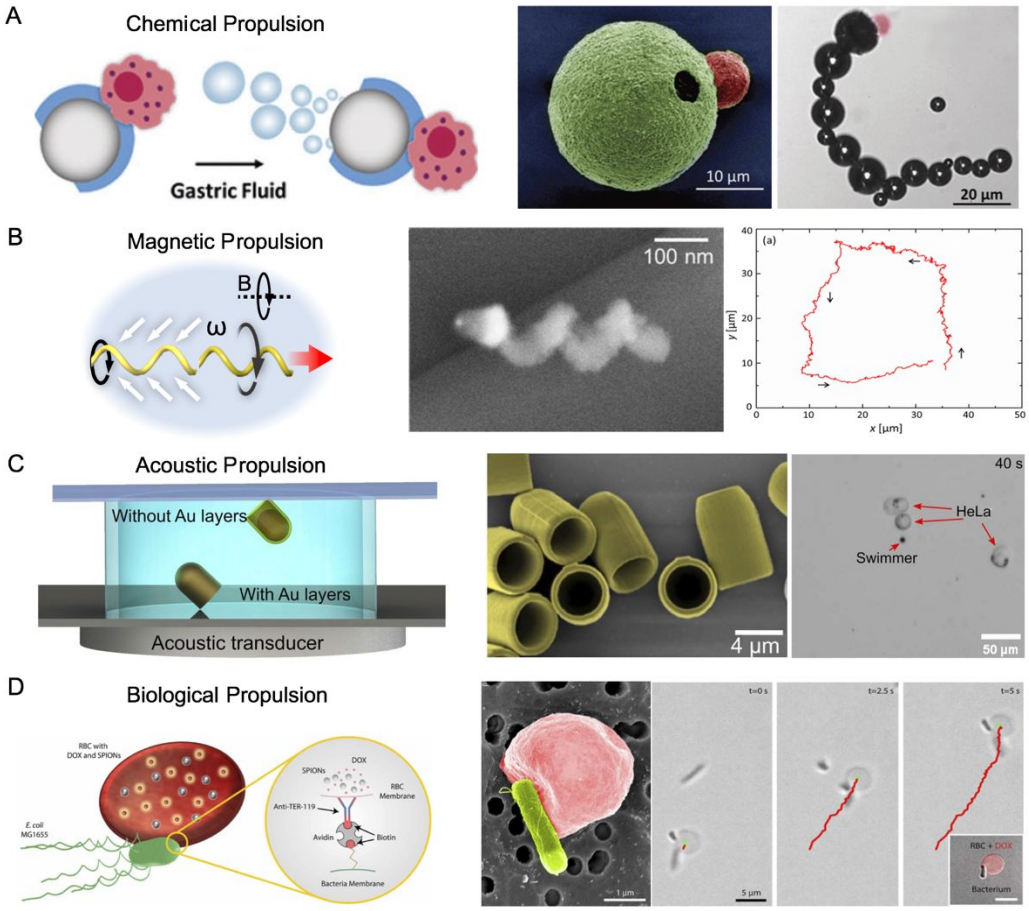

Figure 5. The propulsion mechanisms of the micro/nanorobots in biological fluids. (A) Chemically powered macrophage-hybrid Janus magnesium microrobots modified with macrophage cells. The micromotors are powered by the bubble generated from the reaction between magnesium with water. Reproduced with permission from ref. 196. Copyright 2019 Wiley. (B) Magnetic helical nanorobots fabricated by glancing angle deposition. Their propulsion and motion control in polymeric solution can be realized under external alternative magnetic field. Reproduced with permission from ref. 201. Copyright 2014 American Chemistry Society. (C) Acoustically powered conical microrobots and their motion toward HeLa cells through biofluids. Reproduced with permission from ref. 201. Copyright 2019 American Association for the Advancement of Science. (D) Bacteria and red blood cell-hybrid microrobots and the targeted propulsion toward tumor cells. Reproduced with permission from ref. 205. Copyright 2018 American Association for the Advancement of Science.

guided by an external magnetic field and transport drugs to specified locations (**Fig. 5D**).[205] Bacteria based microrobots, modified with magnetic conical sections, have demonstrated targeted delivery of antibiotics to *E.coli* biofilms via magnetic guidance.[80] Furthermore, sperm driven microrobots have been reported to transport anticancer drug-loaded cargo to tumors *in vitro*.[204]

3.2. Limitations and strategies for propulsion in blood

Blood is a biological fluid containing a high density of dispersed cells. The size and wall shear stress in different blood vessels vary from segments of vessels (**Table 1**).[206-208] The way propulsion of micro/nanoswimmers is altered in blood could vary depending on the size of the swimmer relative to the cells. For swimmers with size smaller or comparable with that of the dispersed cells, the cells may be considered as obstacles for the swimmer. Propulsion of micro/nanoswimmers at this scale resembles the physical picture of propelling in heterogeneous, crowded environments (**Section 2.1**). On the other hand, for swimmers that are considerably larger than the dispersed cells, the swimmers encounter blood as a bulk complex fluid displaying both viscoelasticity (see **Section 2.2**) and shear-thinning rheology (see **Section 2.3**). For swimmers that are considerably larger than the dispersed cells, the swimmers encounter blood as a bulk complex fluid. Impacts on their propulsion performance may then be understood in terms of locomotion in fluids with complex rheology. We discuss below other factors that make efficient and controllable propulsion the blood challenging. Nevertheless, microrobots have been successfully demonstrated to move through blood samples and a number of technical innovations have been reported to enhance their propulsion in this complex medium.[204]

For magnetically propelled microrobots, high levels of ions

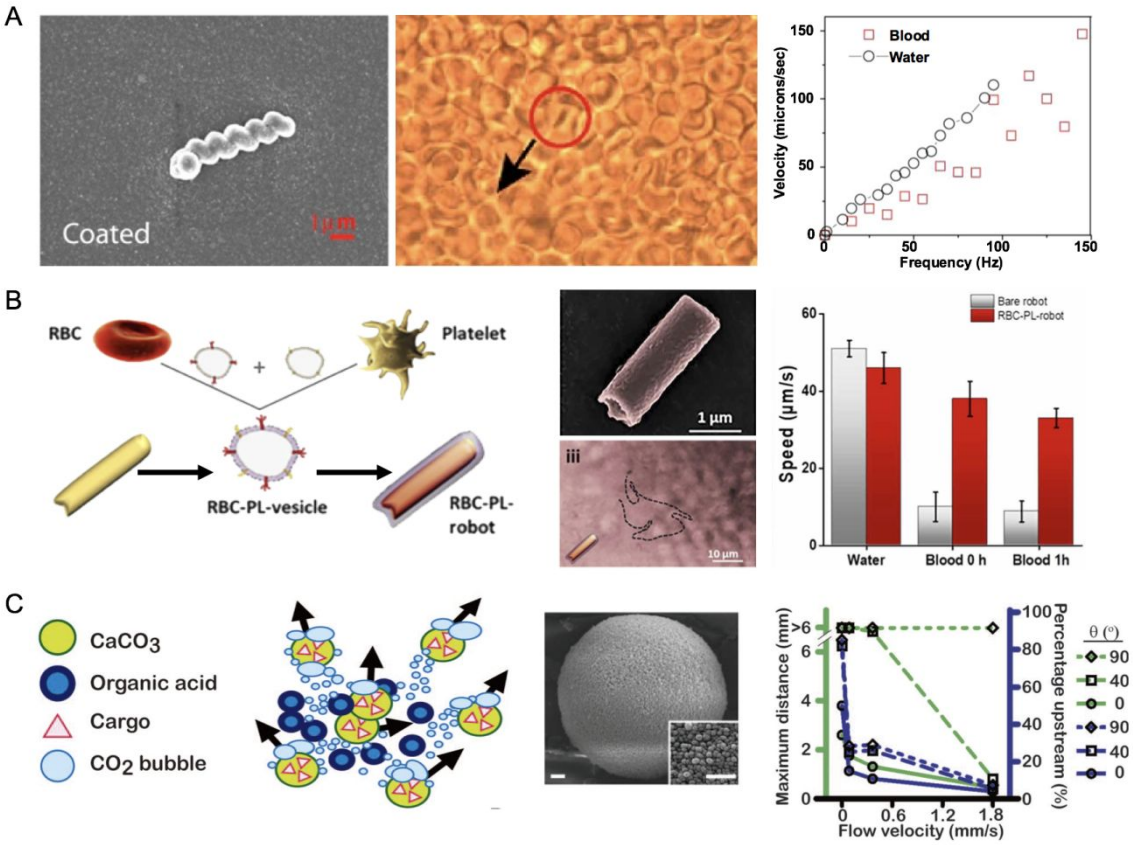

Figure 6. Strategies to enhance the propulsion in blood. (A) Conformal cytocompatible ferrite coatings prevent the etching of magnetic microrobots during operation in whole blood. Reproduced with permission from ref. 209. Copyright 2014 American Chemistry Society. (B) Red blood cell and platelet coating to minimize the protein fouling during operation in blood. Reproduced with permission from ref. 216. Copyright 2018 American Association for the Advancement of Science. (C) Intensively thrusted CO_2 bubble of microrobots accomplish the upstream propulsion in blood. Reproduced with permission from ref. 219. Copyright 2015 American Association for the Advancement of Science.

Table 1. Size and shear stress in human blood vessels.

Vessel	Diameter	Wall thickness	Shear stress (dynes/cm^2)
Artery	~4 mm	~1 mm	10-60
Aorta	~25 mm	~2 mm	Ascending ~12 Descending ~5-8
Veins	~5 mm	~0.5 mm	1-10
Vena cava	~30 mm	~1.5 mm	~5
Venule	~20 μm	~1 μm	~11
Stenotic artery	10-30 μm	2-6 μm	Mildly (>50%) >100, Highly(>90%) >1000
Capillary	5-10 μm	~0.5 μm	~40

(e.g., chloride and phosphate) in the biofluids, particularly human blood, can easily etch their magnetic materials, making a protective anticorrosion coating with long duration in biofluids on the micro/nanorobots crucial for long term operation.[209] It was reported that integrating a conformal ferrite coating onto magnetic micro/nanorobots could be a potential solution which offers unique functionalities for operation in biological fluids, such as high chemical stability, biocompatibility, and propulsion thrust. Importantly, it was found that the ferrite coating was stable over a long period of time in various biofluids (e.g., human blood), and did not significantly affect the propulsion efficiency of such micro/nanorobots (**Fig. 6A**).[209]

For micro/nanorobots, a major challenge to achieve long-lasting propulsion is the biofouling effect, which can change the surface properties of the micromotors and hamper the continuity of local reactions necessary for chemical propulsion. One promising solution is the introduction of biointerfaces such as erythrocyte membranes and platelets, which play an important role in the interaction between natural organisms and biological complex media.[88, 210, 211] Engineering such biointerfaces onto micro/nanorobots has provided an attractive solution to prevent or minimize protein fouling when exposed to blood. To coat the erythrocyte membrane onto micro/nanorobots, the erythrocytes must first undergo hypotonic hemolysis treatment to release the ghost. The resulting erythrocytes ghosts are subsequently forced through 100 nm porous membranes to generate erythrocyte membrane-derived nanovesicles.[212] Erythrocyte nanovesicles are of high surface tension and liable to fuse onto the slide surface; this fusion process retains a bilayer structure of the erythrocyte membrane and maintains the functionality of the

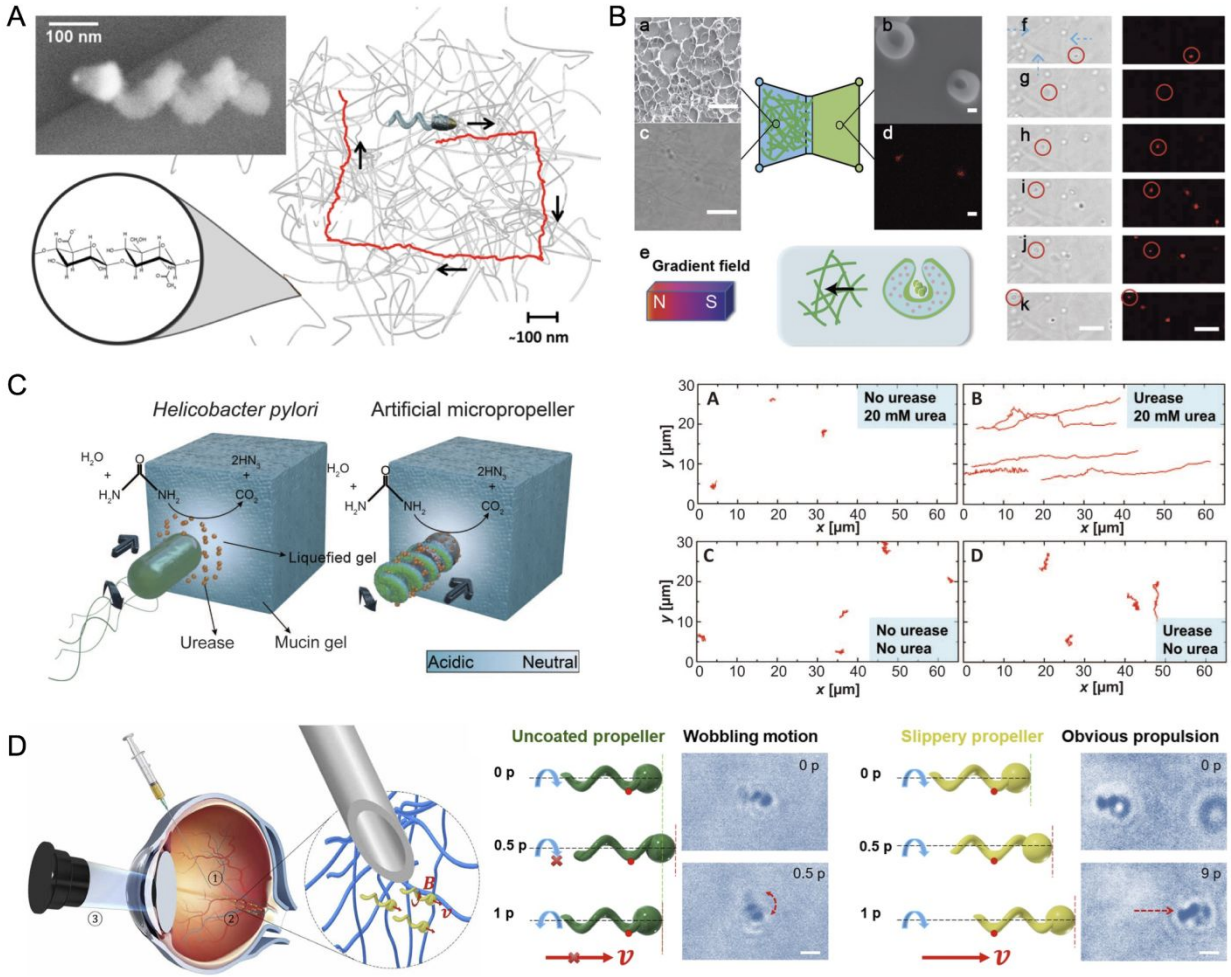

Figure 7. Strategies to enhance the propulsion and penetration in biological porous media. (A) Magnetic helical nanorobots and their controlled propulsion in HA solution under external alternative magnetic field. Reproduced with permission from ref. 201. Copyright 2014 American Chemistry Society. (B) Size effect realize the hydrogen peroxide-powered propulsion of nanorobots through extracellular matrix. Reproduced with permission from ref. 224. Copyright 2017 Wiley. (C) Urease-functionalization achieve the magnetically powered propulsion of magnetically powered helical nanorobot in the mucus through the chemically triggered phase transition of mucus. Reproduced with permission from ref. 227. Copyright 2015 American Association for the Advancement of Science. (D) Combination of size effect and liquid slippery surface endow the intravitreal penetration of magnetically powered nanorobots. Reproduced with permission from ref. 229. Copyright 2018 American Association for the Advancement of Science.

membrane proteins.[213] Taking advantage of the antifouling property of cell membranes and platelets, magnetically powered helical nanorobots and chemically powered Janus magnesium-based microrobots have displayed efficient movement in blood.[196, 214, 215] Combining erythrocyte membranes with platelets, the Wang group demonstrated that dual membrane-hybrid nanorobots sustained prolonged operation in blood (**Fig. 6B**).[216] It should be noted that, it is also possible to engineer cells as the moving motors. For example, by loading magnetic nanoparticles into red blood cells (RBCs), the RBCs can act as ultrasound powered micromotors and their motion can be directed using the external magnetic field.[217, 218]

The circulatory system is an important route for micro/nanorobots for *in vivo* applications, however, navigation in blood flowing at high speeds is still a major challenge. To overcome the issue, intensive gas-generating microrobots consisting of carbonate and tranexamic acid were reported and have the ability to move through aqueous media at speeds of up to 1.5 cm/s and deliver therapeutic payloads into the vasculature of wounds (**Fig. 6C**).[219] Such transportation was enabled through a combination of lateral propulsion, convection, and buoyant rise. The Schmidt group demonstrated another strategy that relies on high propulsion of sperm-based microrobots. The microstructure-loaded sperm microrobots are able to swim against a microchannel-based blood flow model flowing with a high velocity of 0.167 mm/s.[204]

Moving toward many practical applications, micro/nanorobots should be able to seamlessly swim in blood. Despite recent advancements made with propulsion mechanisms and using biointerfaces to avoid etching and fouling, the field must overcome a number of challenges before realizing this goal. In particular, micro/nanorobots must be able

to navigate complex pathways of various sizes in the circulatory system, achieve propulsion under blood pressure, have some means of being imaged**,** and be made with constantly high quality biointerfaces. Improvements have been made with regard to the consistency of biointerface production by noting that most functionalities of cell membranes and platelets including immune evasion, antifouling, and toxin-binding rely on membranes having the right orientation.[220] Considering the different charges between exoplasmic and cytoplasmic sides of erythrocyte membranes and platelets, the right-side-out orientation can be ensured by the functionalization of negatively charged materials prior to the coating.[212] Looking into future, the biohybrid robots with taxis capabilities have the potential to achieve seamless propulsion in whole blood. The magnetically controlled surface rollers or walkers could be another attractive strategy as they could move near the blood vessel. These rollers or walkers exploit the hydrodynamic interaction with the neighboring surfaces to couple rotational and translational motion. Their operation requires the presence of neighboring surfaces and in locations where the flow rate and shear stress is relatively small. The remaining problems, however, must be addressed through new materials and technological innovations to achieve active propulsion in blood. Until then the best these micro/nanorobots can do is hitch a ride on the circulatory system.

3.3. Strategies for enhanced propulsion in biological porous media

The structure of biological porous media, such as mucus, vitreous, and ECM, is mainly composed of a network with various macromolecules such as collagen, water (90-99%), and other molecules. These porous fluids have a wide range of physical properties ranging from soft and viscous to highly elastic. They play crucial roles in the regulation of the mechanical properties of cells and tissues, lubrication of the joints or epithelial and modulation the exchange of different compartments. Associated with a lipid bilayer, they also serve as biological barriers with selective permeability.[221] Particles diffuse with Brownian motion through the network structure and the network feels the influence of steric interactions via the collision of particles and electrostatic interactions from charged particles. Recent research advances in nanotechnology and nanoengineering have led to the development of nanoparticles that can passively diffuse through porous media, however successful delivery of therapeutic agents has not yet been demonstrated. There is thus a need for micro/nanorobots with controllable active motion in biological porous fluid.

Similar to passively diffusing particles, micro/nanorobots in biological porous media must navigate through obstructions present in the macromolecular network. The Nelson group injected a cylindrical microrobot (the outer diameter, 285 μm) *in vivo* in the eye of rabbit model: in the study, vitreous exhibited a viscoelastic behavior, and the microrobot could get caught in collagen fiber bundles.[222] To overcome this issue, the Fischer group demonstrated a size effect-based solution that accomplishes controllable actuation of nanorobots with a size smaller than the mesh size of a porous fluid network (**Fig. 7A**).[201] Although their magnetic helical nanorobots with a filament diameter of about 70 nm could not display directional motion in water owing to the thermal noise, the nanorobots performed such propulsion in viscous solution. The nanorobots were magnetically propelled through hyaluronan solution (HA), which is a good model for a biological porous fluid, and even displayed a higher velocity than in water. In contrast, larger microrobots exhibited slower motion under an external rotating magnetic field. The investigation indicates the efficient actuation of micro/nanorobots in porous fluid requires a threshold size which is decided by the network structure. Helical micro/nanorobots with filament size smaller than the threshold showed considerably elevated propulsion efficiencies, thus demonstrating promise for navigation in biological media and living tissues.[223] The Wilson group developed chemically powered magnetic stomatocyte nanorobots which enabled the penetration of collagen gel (**Fig. 7B**). The stomatocyte nickel-platinum nanorobots used hydrogen peroxide-powered propulsion and were precisely navigated with an external magnetic field. The nanorobots were small enough to be controlled magnetically through the molecular network of collagen gel as a model for tissue.[224]

To better achieve propulsion in biological porous media, recent efforts have shifted towards surface chemistry-based solutions. Biomolecules have been employed to modify micro/nanorobots for enhanced penetration of biological porous media. Mucus, a complex adherent secretion from goblet/mucous cells, is mainly consisted of mucins, proteins, lipids and electrolytes. The mucins fiber form the network of mucus with mesh size of 50-1800 nm, such the glycoprotein mucin combined with electrolytes, lipids and other smaller proteins results in the viscoelastic, lubricating and hydration properties of mucus.[225, 226] One approach takes inspiration from *Helicobacter pylori*, a bacterium that facilitates propulsion in gastric mucus by secreting urease. Ammonia is generated from the catalyzed hydrolysis of urea, which elevates the surrounding pH and lowers the local viscosity. Magnetic helical microrobots have accomplished propulsion in purified porcine mucus via the surface immobilization with urease (**Fig. 7C**).[227] The study indicates the microrobot could successfully navigate through this purified porous fluid, which shows prospect for transporting therapeutic agents across porous media. While these microrobots could perform in purified biological porous media, micro/nanorobots are expected to penetrate raw biological tissues which is much more complex and thus still remain a challenge for the field.

The vitreous of the eye consists of a clear matrix composed of type II collagens, hyaluronic acid, and water. Controllable intravitreal propulsion requires delivery to the posterior part of the eye, the primary therapeutic target for the majority of vision-threating ocular diseases. Microrheology investigations showed that porcine vitreous has a mesh size of around 500 nm.[228] It is expected that the micro/nanomotors with sizes well below the mesh size could move through the porous network if they only experience minimal or negligible adhesion. Recent magnetic micro/nanorobots have been modified with various antiadhesive molecules to achieve intravitreal propulsion.

However, the strategy of integrating a single type of functional molecule onto micro/nanorobots is insufficient to achieve efficient intravitreal propulsion. Molecular modifications make the slippery coating of micro/nanorobots ineffective since macromolecules in the vitreous tend to attach to defects on the coating. A liquid slippery surface, which works similar as the liquid layer on the tropical pitcher plants, was employed on helical nanorobots as a solution to this problem (**Fig. 7D**).[229] The liquid slippery surface modification yields high magnetic intravitreal propulsion by minimizing defects in the coating on micro/nanorobots.

The majority of biological tissues are porous media, like the extracellular matrix (ECM) and mucus which have mesh sizes ranging from several to hundreds of micrometers. Multiple strategies have been developed to realize propulsion in porous media in both model biofluids and raw tissue. Helical nanorobots have achieved propulsion in a porcine eye, but more work must be done to get a comprehensive understanding of active motion in other biological media and tissues. In terms of size effect, we need nanorobots with sizes much smaller than the mesh size of porous fluid. Therefore, to realize propulsion in other tissues, the filament diameter of helical nanorobots needs to be smaller than ~80 nm, which is challenging to fabricate using conventional methods such as two-photon absorption/polymerization and 3D printing. Another strategy is to reduce the interaction between micro/nanorobots and the macromolecular network in porous media by using surface chemistry. In the approach minimizing defects on the surface coating is very important for successful propulsion, since these defects may yield adhesion with the porous fluid network. Currently, one critical issue for clinical translation of this approach is sustaining the anti-adhesion of micro/nanorobots for an extended period of time. Along with this, the intravitreal mobility of the helical nanorobots could be hindered if the magnetic field is turned off then back on as it can slow the adhesion process of gel fibers to the surface of the nanorobots.[229] These challenges must be overcome to realize clinical application.

4. Synthetic micro/nanorobots *in vivo*

In addition to achieving efficient propulsion as described in Sections 2 and 3, synthetic micro/nanorobots face major challenges toward practical medical applications in complex environments. Recent research efforts have led to key advances on evaluating the performance of the micro/nanorobots *in vivo*. We will discuss the promising strategies utilized toward realizing deep tissue imaging (**Section 4.1**) and motion control (**Section 4.2**) of these synthetic micro/nanorobots. Studies in **Section 2** focus on model swimmers in complex yet idealized environments. Examples of recently demonstrated *in vivo* medical applications of these micro/nanorobots will be summarized in **Section 4.3.**

4.1 Imaging of micro/nanorobots *in vivo*

Among the various challenges in biomedical application, imaging of micro/nanorobots is a major one that must be addressed to achieve clinical translation.[230] Images are expected to be of high spatiotemporal resolution, noninvasive, have molecular contrast, and be deeply penetrating to yield precise and reliable micromotor control and navigation. The characteristics of commonly used clinical imaging techniques such as computed tomography (CT), magnetic resonance imaging (MRI), photoacoustic computed imaging (PACT), optical computed imaging (OCT), ultrasound imaging, and fluorescence imaging are listed in **Table 2**.[231-233] Among them, optical imaging facilitates high spatiotemporal resolution and molecular contrast, but its resolution in deep tissue is limited ~1 to 2 mm in depth due to strong optical scattering. To address this issue, a NIR fluorescence-based imaging method was developed for magnetic helical microrobots *in vivo* (**Fig. 8A**). With the maximum transmissivity in the wavelength range of 650–1000 nm, the technique provides the possibility to image microrobots with a high signal-to-noise ratio in the (GI) tract.[234] Fluorescent imaging of magnetic microrobots for active detection of bacterial toxins was reported. Being functionalized with fluorescent sensing probes, the spore-based magnetic microrobots enabled the analysis of *C. diff* toxins by measurement of a fluorescence signal.[235] A reflective microrobot was developed to achieve real-time tracking *ex vivo* taking advantage of the fact that Janus microrobots with half-coated metal layers have high optical reflection. Coupled with IR imaging technology, a single reflective microrobot with a diameter of 20 μm can be tracked in real-time in a glass tube phantom and a mouse skull.[236]

To study the magnetic propulsion of slippery helical nanorobots in the eye, clinical optical coherence tomography (OCT) was employed for the observation of nanorobots close to the retina (**Fig. 8B**). Although the resolution of OCT is too low to resolve the exact features of helical microrobots, it is good enough to track their general location. With the assistance of OCT, the controlled motion of nanorobots in the vitreous of an eye has been demonstrated.[229] More importantly, quantification of OCT results indicates the spatial distribution of the majority of nanorobots were accumulated in the targeted optic disc area with a diameter of ~6 mm, which is better than conventional ocular delivery and thus holds considerable promise for a number of practical ophthalmology uses.

Nuclear imaging techniques involve the use of radionuclides with the goal of heightening sensitivity in imaging studies. It has been reported that X-ray irradiation can be used to observe as well as power the motion of Janus metal microrobot.[237] The Sanchez group successfully tracked catalytic microrobots by applying a combination of X-ray computed tomography (CT) with positron emission tomography (PET).[238] By modifying a gold surface with an iodine isotope, the movement of many chemically powered tubular microrobots in defined channels was monitored in real-time at 1 frame per minute for 15 mins. Other clinical imaging techniques such as ultrasound imaging and fluoresce imaging face limited resolution and contrast for microrobots in tissue. To overcome these issues, considerable efforts have been devoted to real-time visualization of the dynamics of micro/nanorobots with high spatiotemporal

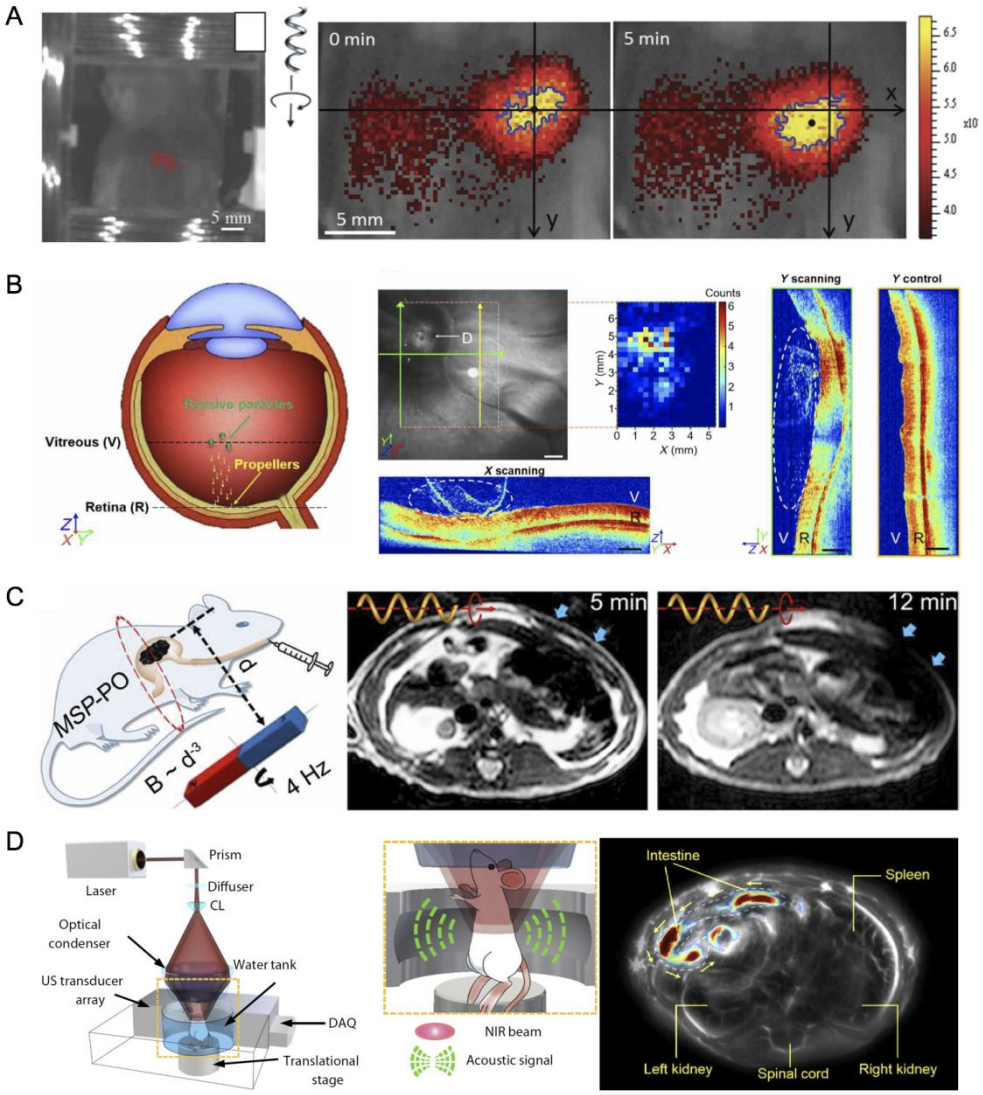

Figure 8. Imaging of the micro/-nanorobots in biological environment. (A) Fluorescence imaging of magnetic helical nanorobots in GI tract *in vivo*. Reproduced with permission from ref. 234. Copyright 2015 Wiley. (B) OCT imaging of accumulation of helical micro/-nanorobots in the retina of eye. Reproduced with permission from ref. 193. Copyright 2018 American Association for the Advancement of Science. (C) MRI imaging of magnetic helical micro/nanorobot *in vivo*. Reproduced with permission from ref. 240. Copyright 2017 American Association for the Advancement of Science. (D) Real time image of the microrobot capsules in the GI tract applying the photoacoustic tomography. Reproduced with permission from ref. 243. Copyright 2019 American Association for the Advancement of Science.

Table 2. Characteristics of various imaging technologies.

	Depth of Penetration	Spatial Resolution	Temporal resolution	Physical principle
MRI	Limitless	25-100 µm	Minutes-hours	Radiowaves
CT	Limitless	50-200 µm	Minutes	X-rays
PET	Limitless	<1 mm	Seconds-minutes	High-energy γ-rays
Ultrasound	1-10 cm	1-2 mm	Seconds-minutes	High-frequency sound wave
PACT	1-7 cm	10-100 µm	Seconds-minutes	Near-infrared light and high-frequency sound wave
OCT	~2 mm	1-15 µm	Seconds-minutes	Visible light
Fluorescence	<1 cm	2-3 mm	Seconds-minutes	Visible or near-infrared light

resolution *in vivo* at the whole-body scale. In a recent study, ultrasound imaging was utilized to track a microrobotic swarm in biofluids. Microrobotic swarms are particularly convenient to image as they are much larger than a small number of

microrobots and can thus be seen with conventional clinical imaging technology.[239].

The combination of magnetic micro/nanorobots with magnetic resonance imaging (MRI) is a logical and promising approach to achieve clinical translation. The Zhang group demonstrated the use of MRI to imaging magnetically powered helical swimmers *in vivo* (**Fig. 8C**). To improve imaging performance, microrobots for injection are separated in peanut oil owing to its higher T_2 signal intensity compared to water. The complex conditions of *in vivo* subcutaneous experiments necessitate a concentration of magnetic microrobot which is ~10 times that of measurements *in vitro*. Cross-sectional MRI imaging can then verify the subcutaneous movement of microrobots in the stomach by comparing the MRI signal to that of peanut oil.[240]

In addition to ultrasound and MRI imaging technologies, photoacoustic tomography (PAT) detects photon-induced ultrasound and provides a high-resolution image at desirable depths of up to 7 centimeters.[241] The Schmidt group demonstrated the tracking of a single microrobot *ex vivo* with the help of Au contrast layers. The microparticles driven by a magnetic field gradient are visualized with PAT in over a centimeter-thick chicken breast as model tissue. Magnetic *Spirulina*-based microrobot was developed using PAT tracking though mice skin, which holds potential promises for theranostics of pathogenic infection.[242] To accomplish real-time imaging under deeper tissue *in vivo*, a microrobotic system has been developed and allows for real-time visualization in the GI tract *in vivo* (**Fig. 8D**).[243] The magnesium-based microrobots with contrasting Au layers were enveloped in an enteric capsule. Such a capsule with microliter to milliliter scale produces a strong photoacoustic signal. Furthermore, PAT imaging could separate abrupt respiratory motion from the microrobots location allowing for precise real-time monitoring in deep tissue *in vivo*.

It should be noticed that most microrobot imaging studies so far were done in ex-vivo tissues or in small animals. Practical imaging technologies with high resolution must be paired with specific micro/nanorobots for efficient *in vivo* application and subsequent clinical translation. Techniques like NIR florescence and nuclear imaging are attractive due to their high spatiotemporal resolution and resolution in deep tissue. It should however be noted that a lower resolution is excusable so long as the general microrobot location can be tracked, as is the case with OCT imaging which showed more specific *in vivo* drug delivery using magnetic robots than current ocular delivery strategies. Nuclear imaging is especially practical as it is deeply penetrating and high molecular contrast but has a low frame rate making real time imaging difficult. Ultrasound is an alternative to nuclear imaging with a faster frame rate however resolution and contrast are comparatively diminished and only microrobotic swarms have been tracked. MRI could provide deep penetration for imaging large animals or human body, but suffer from long data acquisition time. PACT offers high-resolution and high-speed imaging and is particularly suitable for small animal imaging; however, when considering human body imaging, PACT's penetration depth should be further improved. Depending on the specific application of the micro/nanorobots the costs and benefits of each imaging method must be weighed to determine which is the most efficient application.

4.2. Control of micro/nanorobots toward *in vivo* operation

Precise motion control in complex media is essential for the translation of micro/nanorobots to the clinical setting. Micro/nanorobotic approaches have developed a number of diverse strategies to control movement in water through manual operation of physical or chemical triggers including magnetic, ultrasound, thermal, light, and electric controls along with the manipulation of chemical gradients.[244-254]

One promising navigation approach, potentially suitable for *in vivo* biomedical applications, is modification with magnetic materials which allows for controlling robots with an applied magnetic field. Although few examples of such magnetic control have been demonstrated *in vivo*, recent advances show that the velocity, direction, and motion of chemically powered micro/nanorobots can be wirelessly controlled in the body fluids *in vitro*.[252, 255] For example, doxorubicin-incorporated, platinum–nickel-loaded stomatocyte nanomotors displayed magnetotaxis motion and could be guided toward the cancel cell in the HeLa-cell-laden gel matrix using an external magnetic field.[224] Manual navigation is ideal for simple guidance tasks, but traversing complex paths requires a more sophisticated solution. Autopilot navigation has been demonstrated in an *in vitro* study as a potential solution by integrating a system that combines artificial intelligence (AI) based planning with real-time imaging and magnetic control (**Fig. 9A**).[256] The system could automatically detect the obstacles *via* visual recognition, produce obstacle avoidance path planning, and then guide the chemically-powered Janus micromotors along the planned path. It is expected that by designing more sophisticated autopilot systems in combination with the deep tissue imaging and precise magnetic control, future synthetic micro/nanorobots could be able to recognize the dynamically changing environments, overcome nanoscale traffic jams and obstacles *in vivo*, and navigate toward targeted biological area.

Despite the many strategies on micro/nanorobotic control, the majority of studies are limited to the control of a single robot. Considering the limited spatial resolution of imaging techniques under deep tissues, the operation of a single micro/nanorobots is not viable for *in vivo* imaging and operation. Like swimming microorganisms, these micro/nanorobots rarely swim alone but in a group. The collective behavior of active particles, both living systems and artificial swimmers, has attracted substantial interests, because they can generate collective motions and spontaneous flow at a system scale that could be orders of magnitude larger than the scale of the individual particles. We refer readers to comprehensive reviews on the hydrodynamic aspect of collective behaviors of active particles.[257-261] Inspired by the collective intelligence of natural living systems, recent efforts have also been devoted to the control of microrobotic swarms. The He and Xie groups have demonstrated a programed hematite magnetic microrobotic

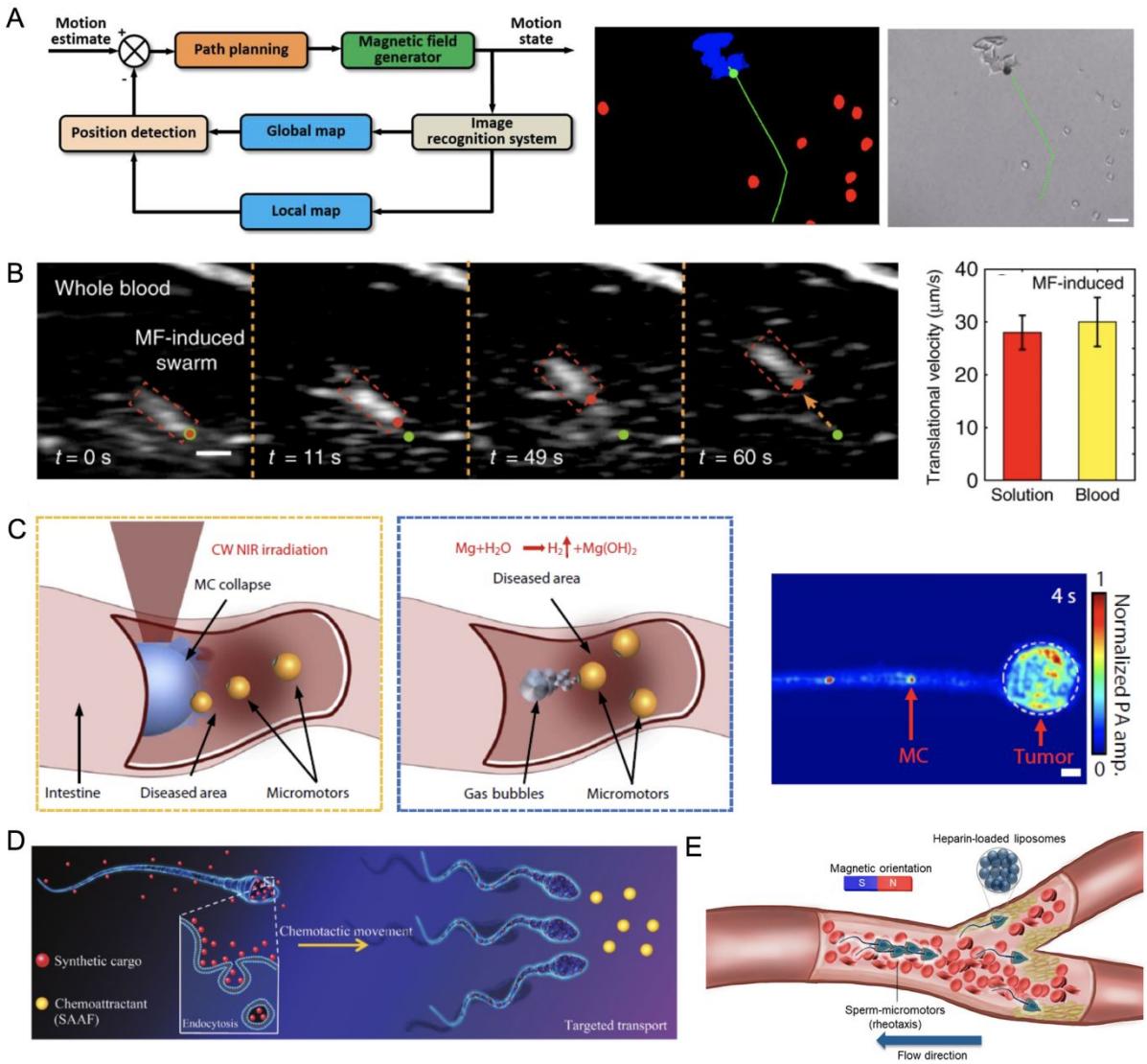

Figure 9. Manipulation of the micro/nanorobots. (A) Autonomous navigation of the Janus micro-/nanorobots in the complex pathway. Reproduced with permission from ref. 256. Copyright 2017 American Chemistry Society. (B) Controllable location in the GI tract through the manipulation of enteric coating onto the microrobots. Reproduced with permission from ref. 239. Copyright 2019 Nature Publishing Group. (C) On-demand accumulation of microrobots toward targeted tumor with the help of photoacoustic imaging. Reproduced with permission from ref. 243. Copyright 2019 American Association for the Advancement of Science. (D and E) Biohybrid approaches for controlling microrobots via chemotaxis (D) and rheotaxis (E). Reproduced with permission from ref. 265. Copyright 2018 Wiley. Reproduced with permission from ref. 204. Copyright 2020 American Chemistry Society.

swarm system. Through the manipulation of an applied magnetic field, the microrobot swarm could switch between various geometries including that of a liquid, chain, ribbon, and vortex.[262] The Zhang group investigated the behavior of magnetic field (MF)-induced micro/nanorobot swarms in various biofluids.[239, 263] They realized the emergence and control of medium and magnetic field-induced microrobot swarm in various biofluids ranging from gastric acid to vitreous humor. The mechanisms involve in magnetic dipolar interaction, hydrodynamic interaction, and self-induced flows at interfaces.[239] The robot swarm under an applied magnetic field was not sensitive to the ion concentrations in the fluid. The MF-induced swarm was stable in fluids with high viscosities and macromolecular network (**Fig. 9B**); in this case, the large microrobot swarm could be imaged with ultrasound and controlled in biological fluids such as blood and vitreous.[239] The microrobot-encapsulated capsule systems provide another promising opportunity for real-time imaging and control *in vivo*.[243] The Gao and Wang groups recently reported a microrobotic system based on the magnesium micromotor-loaded capsules. [243] The capsule was tracked with PAT imaging and broken down via photothermal effects from NIR light after arriving at the target site, which subsequently released the microrobots (**Fig. 9C**).

For example, chemotaxis (**Fig. 9D**) and rheotaxis (**Fig. 9E**) of sperm-based microrobots were recently demonstrated which

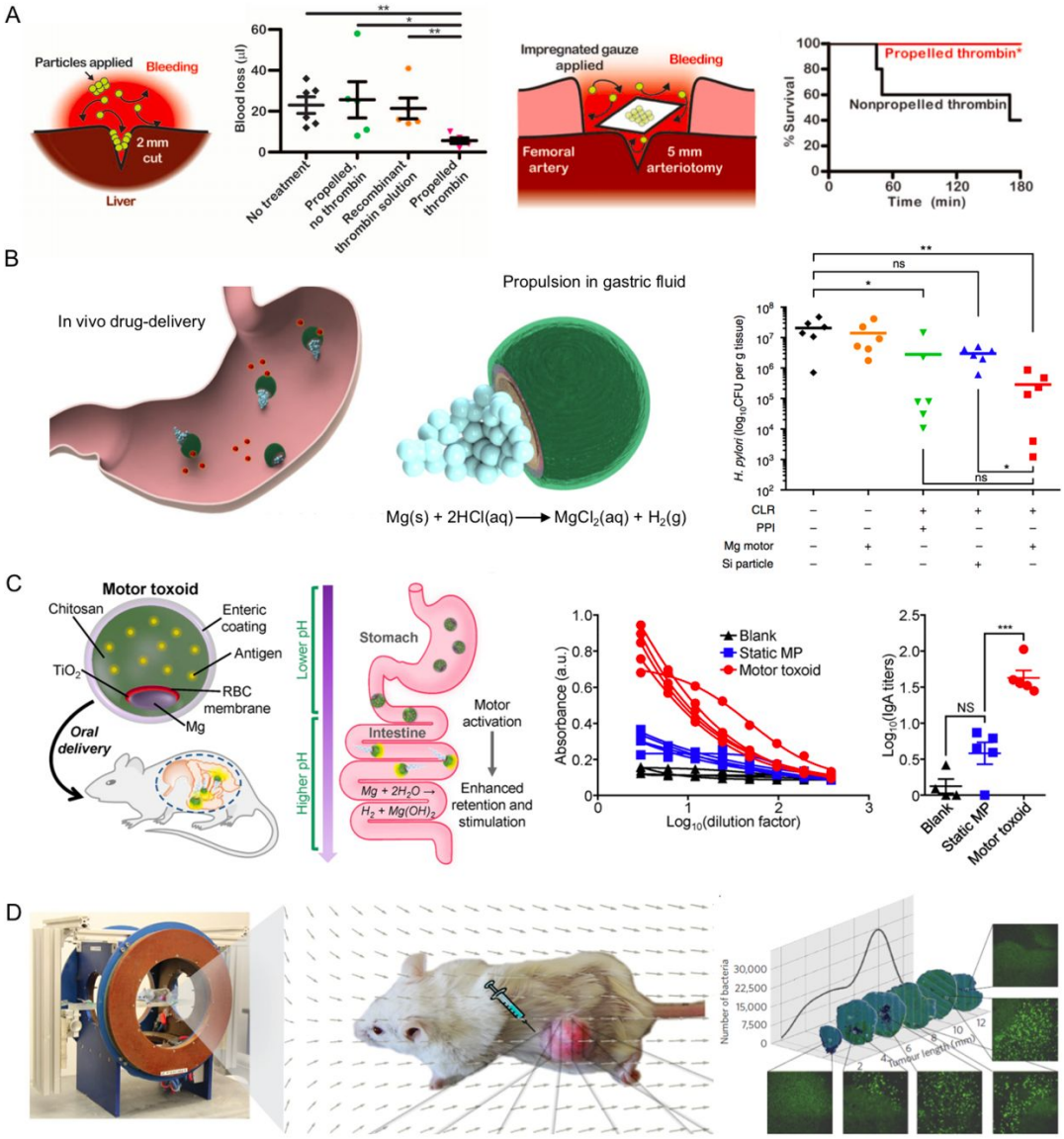

Figure 10. Application of the micro/nanorobots *in vivo*. (A) Treatment of punched liver and femoral artery utilizing coagulation activating thrombin loaded microrobots. The penetration of the micromotors into the wound area could reduce the blood loss and enhance the survival ratio. Reproduced with permission from ref. 219. Copyright 2015 American Association for the Advancement of Science. (B) Stomach infection therapy with ingestible gastric acid driven Mg-based microrobots. The active propulsion of drug-loaded micromotors enhances the tissue penetration and leads to efficient drug delivery with minimized side effects. Reproduced with permission from ref. 268. Copyright 2017 Nature Publishing Group. (C) Active delivery of antigen for oral vaccination using biomimetic micromotors. Reproduced with permission from ref. 271. Copyright 2019 American Chemistry Society. (D) Targeted therapy with bacteria powered microrobots. Reproduced with permission from ref. 274. Copyright 2016 Nature Publishing Group.

could potentially swim against whole blood and deliver therapeutic payloads.[265]

Despite recent advanced on precise and complex control of micro/nanorobots in complex media, challenges for *in vivo* control of these micro/nanoscale robots still exist in many aspects. Heterogeneous properties of biological media typically yield inconsistent velocities and thus hamper precise control *in vivo*. Moreover, the combination of the motion control with *in vivo* imaging technologies is essential for numerous applications given the complex environments in the body. The control of micro/nanorobot swarms or capsules including emergence, manipulation, and reconfiguration, is a promising research direction for clinical translation.

4.3. Medical applications of the micro/nanorobots *in vivo*

One of the primary goals of micro/nanorobots is to transport therapeutic agents to hard to reach tissues. With this in mind, diverse therapeutic investigations employing autonomous micro/nanorobots *in vivo* have been carried out.

The Zhao group reported a nanorobot-based strategy for active thrombolysis *in vivo*; tissue plasminogen activator-loaded nanorobots under magnetic propulsion accelerate the thrombolysis treatment through localized fluid convection which can be manipulated via the strength and frequency of the magnetic field along with the concentration of nanorobots *in vivo*.[266] These particular micro/nanorobots could potentially be applied to treat blood clots in small vessels with further work.[266] Intensive bubble generation from a mixture of $CaCO_3$ and TXA-NH_3^+ has also been employed for self-fueled transportation systems of coagulation enzyme in diverse scenarios (**Fig. 10A**).[219]

One goal for micro/nanorobots is to enhance drug retention *in vivo*. In contrast to the conventional surface modifications, autonomous micro/nanorobots enhance retention without the requirement of complex and specific design for diseased tissues. Ingestible zinc-based microrobots, which could autonomously move in the stomach environment, were firstly evaluated using a mouse model *in vivo*.[267] Gavage administered microrobots exhibited high bubble propulsion in gastric fluid from the chemical reaction between zinc with acid. Such active and efficient propulsion led to greatly enhanced tissue/mucus penetration and thus cargo retention. Of the various micro/nanorobots, magnesium-based microrobots, powered by the magnesium-water reactions, have been widely reported for therapy treatment *in vivo* due to their efficient propulsion in biological media and minimal toxicity.[192, 193] A therapeutic investigation based on active delivery of magnesium-based micro/nanorobots for the treatment of *H. pylori* infection in the stomach was reported (**Fig. 10B**). The evaluation of the therapeutic efficacy of clinical doses of the drug-loaded microrobots *in vivo* indicated elevated delivery efficacy and reduced bacterial burden when compared with passive therapeutic carriers.[268] Another therapeutic use of magnesium-based microrobots in the stomach is to adjust local physiological conditions (e.g., neutralizing the stomach pHs) of the gastric fluid to facilitate the pH-triggered drug release. Coupling the reaction of magnesium and gastric acid with local fluid convection from active motion results in the rapid proton depletion from the microrobots without side effect and offers considerable promises for proton pump inhabitation and controllable release.[269] In addition to these bubble propelled micromotors, the magnetically driven nanorobots were also successfully applied in vivo to reduce tumor growth in rodent models.[270]

In addition to targeted drug delivery, active vaccine delivery is an important therapeutic application (this could be particularly important as it aids the prevention of infectious diseases given the recent pandemic of COVID-19). As an example, magnesium-based microrobot toxoids were developed and utilized for oral vaccination. A toxin-inserted erythrocyte membrane coating onto the microrobots enabled neutralization of the toxic antigenic payloads and induced the mucosal immunity (**Fig. 10C**).[271] The intestinal localization from mucoadhesive and enteric coating of microrobots then simulates an invasive infection. The propulsion of the microrobots in the GI tract enhanced the retention and uptake of antigenic agents *in vivo*, indicating the benefits of using such micro/nanorobots as delivery vehicles compared to conventional nanoparticles.

Bacteria and sperm-hybrid robots are promising candidate for micro/nanorobot-based active delivery as they hold unique antigenic and transport properties that artificial micro/nanorobots do not have. For instance, sperm driven micro/nanorobots have been developed to transport a drug-loaded polymer cargo to a model tumor spheroid *in vitro*.[272] Benefiting from the rheotaxis behavior and high propulsion of sperm, the sperm-based microrobot can swim against blood flow for active delivery.[204] Active delivery strategies were demonstrated with bacteria-hybrid microrobots with multifunctional cargo such as microcapsules and erythrocyte. The drug-encapsulated polymer microcapsule with a size of 1 μm was driven by *E. coli* and transported to targeted breast cancer cells *in vitro* under external magnetic guidance.[273] To improve the performance of the cargo, magnetic nanoparticles and drug-loaded erythrocytes were functionalized onto *E. coil* as cargo through biotin-avidin binding. Sharing the biofunctional features of bacteria and erythrocyte, the bacteria and erythrocyte-hybrid possess optimal motility and deformability for targeted biomedical applications.[205] Given to the hypoxic nature of tumorous regions, magnetotactic bacteria-hybrid microrobots carrying drug-loaded nanoliposomes can be applied for target delivery using the magneto-aerotactic migration behavior from bacteria (**Fig. 10D**).[274]

As described above, there is great potential for micro/nanorobots to target diseased sites, but several limitations must first be addressed. Actuation in complex media, penetration of biological tissues, imaging and control under deep tissues to name a few. Enhanced retention is another potential benefit that utilizes the propulsion function of the micro/nanorobots which provides a universal but robust strategy for a wide range of treatments. Particularly with a full platform which integrates real-time visualization and reconfigurable swarms, micro/nanorobots can have a big impact is local disease treatment.

5. Conclusion and outlook

In summary, we have discussed and highlighted here the recent advances in micro/nanorobots toward operation in complex fluids. Over the past few decades, a number of theoretical and experimental studies lead to the development of various micro/nanorobots that can be propelled by different mechanisms (powered by various external fields or local chemical fuels). Considering the practical biomedical use, realistic biological environments are substantially more complex than ideal Newtonian fluids. In recent years, researchers have started to make progress on investigating the influences of fluid complexities that can arise in more realistic biological systems, including environmental heterogeneity and non-Newtonian behaviors (shear-thinning and viscoelastic

effects) of biological fluids. A number of materials and engineering innovations have been reported to achieve efficient propulsion of the micro/nanorobots in various complex fluids ranging from blood to porous media (e.g., mucus and vitreous). Owing to the major advances over developing efficient and multifunctional micro/nanorobots that could operate in complex biofluids, the proof-of-concept in vivo therapeutic applications have been demonstrated recently (examples include treating blood clots, bacterial infection, as well as cancers). Despite the significant progress in this emerging field, a number of challenges remain to be addressed in order to fulfill the full potential of synthetic micro/nanorobots in biomedicine.

Considering that the biological fluids are typically both shear-thinning and viscoelastic, our understanding on the complex interactions of these non-Newtonian behaviors and their influence to the propulsion of micro/nanorobots is still very limited. From the design aspects of swimming micro/nanorobots, a number of factors including the speed fluctuations, scattering and trapping dynamics in the presence of various biofluid obstacles and their swimming performance in shear-thinning and viscoelastic fluids should be carefully considered. New functional materials and propulsion mechanisms more suitable for operation in complex fluids (particularly blood, mucus, vitreous and other extracellular matrix) are strongly desired for next-generation micro/nanorobots. Moreover, mass-production approach for high-performance and low-cost biomedical micro/nanorobots should be explored toward practical clinical applications; recent examples of 3D printing, two-photon polymerization, as well as glancing angle deposition show great promise for large scale preparation of synthetic micro/nanorobots.

In vivo applications and future clinical operations of the micro/nanorobots usually require real-time deep tissue imaging and guidance which are still significantly under developed. Recently through interdisciplinary collaborations, advanced imaging technologies including MRI, ultrasound, OCT, as well as PAT have been explored to track the microrobots *in vivo*. Considering the small size of an individual microrobot, current imaging demonstrations focus on the microrobot swarm. Imaging and control of a signal robot under deep tissue require further materials and technology development. With the assistance of in vivo imaging, one could control the operation of microrobots using various external controls via magnetic, ultrasound or optical fields. Another attractive method for in vivo robot control is creating the intelligent motors that could respond to surrounding environment variations (such as temperature or molecule gradients) and achieve self-navigation in complex environments.[275-277]

While addressing the challenges of propulsion and control in complex fluids, we should expand the application scope of micro/nanorobots. In this regard, micro/nanorobots with versatile functionality and targeting moieties need to be developed to perform complex tasks and evaluated *in vivo* for different health conditions. In addition to the therapeutic efficacy, the *in vivo* toxicity, biocompatibility, and biodegradability of the micro/nanorobots need to be carefully examined and considered during robot design and evaluation stages. It is worth noting that in many practical medical application occasions, the swarms of micro/nanorobots display significant benefit for both *in vivo* imaging and control. The cooperative action and coordinated movement of micro/nanorobots are promising for enhancing the capacity of advanced transport and targeted drug delivery.

We envision that further research progress and future clinical translation of the emerging micro/nanorobots require interdisciplinary collaborative efforts among materials scientists, chemists, fluid mechanicians, imaging and medical experts. Although the field of micro/nanorobotics is still in the infancy, it is receiving dramatically increased attention across different fields over the past decades. With continuing materials and technological innovations, the micro/nanorobots will prove to be of great importance for numerous medical applications; the Fantastic voyage vision will be eventually fulfilled by these tiny multifunctional swimming micro/nanorobots.

Conflicts of interest

There are no conflicts to declare.

Acknowledgements

This work was supported by National Science Foundation grants 1931214 (to W.G.), 1830958 and 1931292 (to O.S.P.) and the Donna and Benjamin M. Rosen Bioengineering Center at California Institute of Technology (to W.G.).

Notes and references

1 J. Wang and W. Gao, *ACS Nano*, 2012, **6**, 5745-5751.
2 G. Z. Yang, J. Bellingham, P. E. Dupont, P. Fischer, L. Floridi, R. Full, N. Jacobstein, V. Kumar, M. McNutt, R. Merrifield, B. J. Nelson, B. Scassellati, M. Taddeo, R. Taylor, M. Veloso, Z. L. Wang and R. Wood, *Sci. Robot.*, 2018, **3**, eaar7650.
3 P. Fischer, B. J. Nelson and G. Z. Yang, *Sci. Robot.*, 2018, **3**, eaau0448.
4 M. Sitti, *Nat. Rev. Mater.*, 2018, **3**, 74-75.
5 Y. Mei, A. A. Solovev, S. Sanchez and O. G. Schmidt, *Chem. Soc. Rev.*, 2011, **40**, 2109-2119.
6 E. M. Purcell, *Am. J. Phys.*, 1977, **45**, 3-11.
7 O. S. Pak and E. Lauga, in *Fluid-structure interactions in low-Reynolds-number flows*, The Royal Society of Chemistry, 2015, pp. 100-167.
8 L. J. Fauci and R. Dillon, *Ann. Rev. Fluid Mech.*, 2006, **38**, 371-394.
9 J. M. Yeomans, D. O. Pushkin and H. Shum, *EPL*, 2014, **223**, 1771-1785.
10 E. Lauga and T. R. Powers, *Rep. Prog. Phys.*, 2009, **72**, 096601.
11 J. Elgeti, R. G. Winkler and G. Gompper, *Rep. Prog. Phys.*, 2015, **78**, 056601.
12 E. Lauga, *Ann. Rev. Fluid Mech.*, 2016, **48**, 105-130.
13 C. Bechinger, R. Di Leonardo, H. Lowen, C. Reichhardt, G. Volpe and G. Volpe, *Rev. Mod. Phys.*, 2016, **88**, 045006.
14 A. E. Patteson, A. Gopinath and P. E. Arratia, *Curr. Opin. Colloid Interface Sci.*, 2016, **21**, 86-96.
15 C. Datt, G. Natale, S. G. Hatzikiriakos and G. J. Elfring, *J. Fluid Mech.*, 2017, **823**, 675-688.

16 M. Sitti and D. S. Wiersma, *Adv. Mater.*, 2020, **32**, e1906766.
17 J. Li, B. Esteban-Fernandez de Avila, W. Gao, L. Zhang and J. Wang, *Sci. Robot.*, 2017, **2**, eaam6431.
18 B. Esteban-Fernández de Ávila, P. Angsantikul, J. Li, W. Gao, L. Zhang and J. Wang, *Adv. Funct. Mater.*, 2018, **28**, 1705640.
19 W. Gao, A. Pei and J. Wang, *ACS Nano*, 2012, **6**, 8432-8438.
20 M. Medina-Sanchez, H. Xu and O. G. Schmidt, *Ther. Deliv.*, 2018, **9**, 303-316.
21 T. Patino, X. Arque, R. Mestre, L. Palacios and S. Sanchez, *Acc. Chem. Res.*, 2018, **51**, 2662-2671.
22 T. E. Mallouk and A. Sen, *Sci. Am.*, 2009, **300**, 72-77.
23 F. Novotný, H. Wang and M. Pumera, *Chem*, 2020, **6**, 867-884.
24 M. Luo, Y. Z. Feng, T. W. Wang and J. G. Guan, *Adv. Funct. Mater.*, 2018, **28**, 1706100.
25 X. Lin, Z. Wu, Y. Wu, M. Xuan and Q. He, *Adv. Mater.*, 2016, **28**, 1060-1072.
26 T. Xu, W. Gao, L. P. Xu, X. Zhang and S. Wang, *Adv. Mater.*, 2017, **29**, 1603250.
27 R. Dreyfus, J. Baudry, M. L. Roper, M. Fermigier, H. A. Stone and J. Bibette, *Nature*, 2005, **437**, 862-865.
28 W. Gao, S. Sattayasamitsathit, K. M. Manesh, D. Weihs and J. Wang, *J. Am. Chem. Soc.*, 2010, **132**, 14403-14405.
29 O. S. Pak, W. Gao, J. Wang and E. Lauga, *Soft Matter*, 2011, **7**, 8169-8181.
30 W. Gao, D. Kagan, O. S. Pak, C. Clawson, S. Campuzano, E. Chuluun-Erdene, E. Shipton, E. E. Fullerton, L. Zhang, E. Lauga and J. Wang, *Small*, 2012, **8**, 460-467.
31 S. Tottori, L. Zhang, F. Qiu, K. K. Krawczyk, A. Franco-Obregon and B. J. Nelson, *Adv. Mater.*, 2012, **24**, 811-816.
32 L. Zhang, J. J. Abbott, L. X. Dong, B. E. Kratochvil, D. Bell and B. J. Nelson, *Appl. Phys. Lett.*, 2009, **94**, 064107.
33 A. Ghosh and P. Fischer, *Nano Lett.*, 2009, **9**, 2243-2245.
34 T. L. Li, A. N. Zhang, G. B. Shao, M. S. Wei, B. Guo, G. Y. Zhang, L. Q. Li and W. Wang, *Adv. Funct. Mater.*, 2018, **28**, 1706066.
35 X. H. Yan, Q. Zhou, J. F. Yu, T. T. Xu, Y. Deng, T. Tang, Q. Feng, L. M. Bian, Y. Zhang, A. Ferreira and L. Zhang, *Adv. Funct. Mater.*, 2015, **25**, 5333-5342.
36 T. T. Xu, Y. M. Guan, J. Liu and X. Y. Wu, *IEEE Trans. Autom. Sci. Eng.*, 2020, **17**, 325-333.
37 Y. Liu, G. Li, H. Lu, Y. Yang, Z. Liu, W. Shang and Y. Shen, *ACS Appl. Mater. Interfaces*, 2019, **11**, 25664-25673.
38 T. Qiu, S. Palagi, J. Sachs and P. Fischer, *IEEE Int. Conf. Robot. Autom.*, 2018, 3595-3600.
39 R. Mhanna, F. Qiu, L. Zhang, Y. Ding, K. Sugihara, M. Zenobi-Wong and B. J. Nelson, *Small*, 2014, **10**, 1953-1957.
40 G. Loget, D. Zigah, L. Bouffier, N. Sojic and A. Kuhn, *Acc. Chem. Res.*, 2013, **46**, 2513-2523.
41 G. Loget and A. Kuhn, *Nat. Commun.*, 2011, **2**, 535.
42 G. Loget and A. Kuhn, *J. Am. Chem. Soc.*, 2010, **132**, 15918-15919.
43 L. Ren, D. Zhou, Z. Mao, P. Xu, T. J. Huang and T. E. Mallouk, *ACS Nano*, 2017, **11**, 10591-10598.
44 S. Ahmed, W. Wang, L. Bai, D. T. Gentekos, M. Hoyos and T. E. Mallouk, *ACS Nano*, 2016, **10**, 4763-4769.
45 D. Ahmed, M. Lu, A. Nourhani, P. E. Lammert, Z. Stratton, H. S. Muddana, V. H. Crespi and T. J. Huang, *Sci. Rep.*, 2015, **5**, 9744.
46 A. L. Balk, L. O. Mair, P. P. Mathai, P. N. Patrone, W. Wang, S. Ahmed, T. E. Mallouk, J. A. Liddle and S. M. Stavis, *ACS Nano*, 2014, **8**, 8300-8309.
47 V. Garcia-Gradilla, J. Orozco, S. Sattayasamitsathit, F. Soto, F. Kuralay, A. Pourazary, A. Katzenberg, W. Gao, Y. Shen and J. Wang, *ACS Nano*, 2013, **7**, 9232-9240.
48 V. Garcia-Gradilla, S. Sattayasamitsathit, F. Soto, F. Kuralay, C. Yardimci, D. Wiitala, M. Galarnyk and J. Wang, *Small*, 2014, **10**, 4154-4159.
49 D. Kagan, M. J. Benchimol, J. C. Claussen, E. Chuluun-Erdene, S. Esener and J. Wang, *Angew. Chem. Int. Ed.*, 2012, **51**, 7519-7522.
50 H. R. Jiang, N. Yoshinaga and M. Sano, *Phys. Rev. Lett.*, 2010, **105**, 268302.
51 A. P. Bregulla, H. Yang and F. Cichos, *ACS Nano*, 2014, **8**, 6542-6550.
52 B. Qian, D. Montiel, A. Bregulla, F. Cichos and H. Yang, *Chem. Sci.*, 2013, **4**, 1420-1429.
53 L. Kong, C. C. Mayorga-Martinez, J. Guan and M. Pumera, *ACS Appl. Mater. Interfaces*, 2018, **10**, 22427-22434.
54 V. Sridhar, B. W. Park and M. Sitti, *Adv. Funct. Mater.*, 2018, **28**, 1704902.
55 W. Li, X. R. Wu, H. Qin, Z. Q. Zhao and H. W. Liu, *Adv. Funct. Mater.*, 2016, **26**, 3164-3171.
56 Y. J. Wu, T. Y. Si, J. X. Shao, Z. G. Wu and Q. He, *Nano Res.*, 2016, **9**, 3747-3756.
57 Z. Wu, T. Si, W. Gao, X. Lin, J. Wang and Q. He, *Small*, 2016, **12**, 577-582.
58 J. Li, T. Li, T. Xu, M. Kiristi, W. Liu, Z. Wu and J. Wang, *Nano Lett.*, 2015, **15**, 4814-4821.
59 H. Wang and M. Pumera, *Chem. Rev.*, 2015, **115**, 8704-8735.
60 H. Wang and M. Pumera, *Nanoscale*, 2017, **9**, 2109-2116.
61 Y. F. Mei, G. S. Huang, A. A. Solovev, E. B. Urena, I. Moench, F. Ding, T. Reindl, R. K. Y. Fu, P. K. Chu and O. G. Schmidt, *Adv. Mater.*, 2008, **20**, 4085-4090.
62 J. Katuri, X. Ma, M. M. Stanton and S. Sanchez, *Acc. Chem. Res.*, 2017, **50**, 2-11.
63 W. Gao, S. Sattayasamitsathit, J. Orozco and J. Wang, *J. Am. Chem. Soc.*, 2011, **133**, 11862-11864.
64 S. Sanchez, A. A. Solovev, Y. Mei and O. G. Schmidt, *J. Am. Chem. Soc.*, 2010, **132**, 13144-13145.
65 A. A. Solovev, Y. Mei and O. G. Schmidt, *Adv. Mater.*, 2010, **22**, 4340-4344.
66 Y. Wu, Z. Wu, X. Lin, Q. He and J. Li, *ACS Nano*, 2012, **6**, 10910-10916.
67 Z. Wu, X. Lin, Y. Wu, T. Si, J. Sun and Q. He, *ACS Nano*, 2014, **8**, 6097-6105.
68 W. F. Paxton, K. C. Kistler, C. C. Olmeda, A. Sen, S. K. St Angelo, Y. Cao, T. E. Mallouk, P. E. Lammert and V. H. Crespi, *J. Am. Chem. Soc.*, 2004, **126**, 13424-13431.
69 T. R. Kline, W. F. Paxton, T. E. Mallouk and A. Sen, *Angew. Chem. Int. Ed.*, 2005, **44**, 744-746.
70 J. Li, J. Zhang, W. Gao, G. Huang, Z. Di, R. Liu, J. Wang and Y. Mei, *Adv. Mater.*, 2013, **25**, 3715-3721.
71 W. Gao, A. Pei, R. Dong and J. Wang, *J. Am. Chem. Soc.*, 2014, **136**, 2276-2279.
72 R. Laocharoensuk, J. Burdick and J. Wang, *ACS Nano*, 2008, **2**, 1069-1075.
73 J. L. Moran and J. D. Posner, *Ann. Rev. Fluid Mech.,* 2017, **49**, 511-540.
74 J. Moran and J. Posner, *Phys. Today*, 2019, **72**, 44-50.
75 C. Gao, Z. Lin, D. Wang, Z. Wu, H. Xie and Q. He, *ACS Appl. Mater. Interfaces*, 2019, **11**, 23392-23400.
76 C. Y. Gao, Z. H. Lin, X. K. Lin and Q. He, *Adv. Ther.*, 2018, **1**, 1800056.
77 V. Magdanz, S. Sanchez and O. G. Schmidt, *Adv. Mater.*, 2013, **25**, 6581-6588.
78 H. Zhang, Z. Li, Z. Wu and Q. He, *Adv. Ther.*, 2019, **2**, 1900096.
79 D. Ahmed, T. Baasch, N. Blondel, N. Laubli, J. Dual and B. J. Nelson, *Nat. Commun.*, 2017, **8**, 770.
80 M. M. Stanton, B. W. Park, D. Vilela, K. Bente, D. Faivre, M. Sitti and S. Sanchez, *ACS Nano*, 2017, **11**, 9968-9978.
81 M. M. Stanton, B. W. Park, A. Miguel-Lopez, X. Ma, M. Sitti and S. Sanchez, *Small*, 2017, **13**, 1603679.
82 L. Zhang, T. Petit, Y. Lu, B. E. Kratochvil, K. E. Peyer, R. Pei, J. Lou and B. J. Nelson, *ACS Nano*, 2010, **4**, 6228-6234.

83 C. E. Sing, L. Schmid, M. F. Schneider, T. Franke and A. Alexander-Katz, *Proc. Natl. Acad. Sci. U. S. A.*, 2010, **107**, 535-540.
84 J. Han, J. Zhen, V. Du Nguyen, G. Go, Y. Choi, S. Y. Ko, J. O. Park and S. Park, *Sci. Rep.*, 2016, **6**, 28717.
85 Y. Alapan, O. Yasa, B. Yigit, I. C. Yasa, P. Erkoc and M. Sitti, *Annu. Rev. Contr. Robot. Auton. Syst.*, 2019, **2**, 205-230.
86 B. Yigit, Y. Alapan and M. Sitti, *Adv. Sci.*, 2019, **6**, 1801837.
87 T. O. Tasci, P. S. Herson, K. B. Neeves and D. W. Marr, *Nat. Commun.*, 2016, **7**, 10225.
88 B. Esteban-Fernandez de Avila, W. Gao, E. Karshalev, L. Zhang and J. Wang, *Acc. Chem. Res.*, 2018, **51**, 1901-1910.
89 Y. Tu, F. Peng, A. Adawy, Y. Men, L. K. Abdelmohsen and D. A. Wilson, *Chem. Rev.*, 2016, **116**, 2023-2078.
90 F. Peng, Y. Tu and D. A. Wilson, *Chem. Soc. Rev.*, 2017, **46**, 5289-5310.
91 J. Li, B. Esteban-Fernandez de Avila, W. Gao, L. Zhang and J. Wang, *Sci. Robot.*, 2017, **2**, eaam6431.
92 W. Gao and J. Wang, *Nanoscale*, 2014, **6**, 10486-10494.
93 M. Medina-Sanchez and O. G. Schmidt, *Nature*, 2017, **545**, 406-408.
94 G. Li and J. X. Tang, *Phys. Rev. Lett.*, 2009, **103**, 078101.
95 E. Lauga, W. R. DiLuzio, G. M. Whitesides and H. A. Stone, *Biophys. J.*, 2006, **90**, 400-412.
96 A. P. Berke, L. Turner, H. C. Berg and E. Lauga, *Phys. Rev. Lett.*, 2008, **101**, 038102.
97 K. Drescher, J. Dunkel, L. H. Cisneros, S. Ganguly and R. E. Goldstein, *Proc. Natl. Acad. Sci. U. S. A.*, 2011, **108**, 10940-10945.
98 J. W. Costerton, P. S. Stewart and E. P. Greenberg, *Science*, 1999, **284**, 1318-1322.
99 P. Denissenko, V. Kantsler, D. J. Smith and J. Kirkman-Brown, *Proc. Natl. Acad. Sci. U. S. A.*, 2012, **109**, 8007-8010.
100 A. Guidobaldi, Y. Jeyaram, I. Berdakin, V. V. Moshchalkov, C. A. Condat, V. I. Marconi, L. Giojalas and A. V. Silhanek, *Phys. Rev. E*, 2014, **89**, 032720.
101 N. Heddergott, T. Kruger, S. B. Babu, A. Wei, E. Stellamanns, S. Uppaluri, T. Pfohl, H. Stark and M. Engstler, *PLoS Pathog.*, 2012, **8**, e1003023.
102 J. Rutllant, M. Lopez-Bejar and F. Lopez-Gatius, *Reprod. Domest. Anim.*, 2005, **40**, 79-86.
103 G. Juarez, K. Lu, J. Sznitman and P. E. Arratia, *Europhys. Lett.*, 2010, **92**, 44002.
104 S. Jung, *Phys. Fluids*, 2010, **22**, 031903.
105 A. M. Leshansky, *Phys. Rev. E*, 2009, **80**, 051911.
106 N. Ho, S. D. Olson and K. Leiderman, *Phys. Rev. E*, 2016, **93**, 043108.
107 K. Leiderman and S. D. Olson, *Phys. Fluids*, 2016, **28**, 021902.
108 S. A. Mirbagheri and H. C. Fu, *Phys. Rev. Lett.*, 2016, **116**, 198101.
109 H. Nganguia and O. S. Pak, *J. Fluid Mech.*, 2018, **855**, 554-573.
110 N. Ho, K. Leiderman and S. Olson, *J. Fluid Mech.*, 2019, **864**, 1088-1124.
111 H. C. Fu, V. B. Shenoy and T. R. Powers, *Europhys. Lett.*, 2010, **91**, 24002.
112 J. K. Wróbel, S. Lynch, A. Barrett, L. Fauci and R. Cortez, *J. Fluid Mech.*, 2016, **792**, 775-797.
113 S. E. Spagnolie and E. Lauga, *J. Fluid Mech.*, 2012, **700**, 105-147.
114 D. Takagi, J. Palacci, A. B. Braunschweig, M. J. Shelley and J. Zhang, *Soft Matter*, 2014, **10**, 1784-1789.
115 O. Sipos, K. Nagy, R. Di Leonardo and P. Galajda, *Phys. Rev. Lett.*, 2015, **114**, 258104.
116 S. E. Spagnolie, G. R. Moreno-Flores, D. Bartolo and E. Lauga, *Soft Matter*, 2015, **11**, 3396-3411.
117 A. T. Brown, I. D. Vladescu, A. Dawson, T. Vissers, J. Schwarz-Linek, J. S. Lintuvuori and W. C. Poon, *Soft Matter*, 2016, **12**, 131-140.
118 G. Volpe, I. Buttinoni, D. Vogt, H. J. Kummerer and C. Bechinger, *Soft Matter*, 2011, **7**, 8810-8815.
119 J. Su, H. Jiang and Z. Hou, *Soft Matter*, 2019, **15**, 6830-6835.
120 J. Simmchen, J. Katuri, W. E. Uspal, M. N. Popescu, M. Tasinkevych and S. Sanchez, *Nat. Commun.*, 2016, **7**, 10598.
121 M. S. D. Wykes, X. Zhong, J. J. Tong, T. Adachi, Y. P. Liu, L. Ristroph, M. D. Ward, M. J. Shelley and J. Zhang, *Soft Matter*, 2017, **13**, 4681-4688.
122 M. Contino, E. Lushi, I. Tuval, V. Kantsler and M. Polin, *Phys. Rev. Lett.*, 2015, **115**, 258102.
123 V. Kantsler, J. Dunkel, M. Polin and R. E. Goldstein, *Proc. Natl. Acad. Sci. U. S. A.*, 2013, **110**, 1187-1192.
124 E. Lushi, V. Kantsler and R. E. Goldstein, *Phys. Rev. E*, 2017, **96**, 023102.
125 S. E. Spagnolie, C. Wahl, J. Lukasik and J. L. Thiffeault, *Physica D*, 2017, **341**, 33-44.
126 M. Jabbarzadeh, Y. Hyon and H. C. Fu, *Phys. Rev. E*, 2014, **90**, 043021.
127 A. Kamal and E. E. Keaveny, *J. R. Soc. Interface*, 2018, **15**, 20180592.
128 T. Jakuszeit, O. A. Croze and S. Bell, *Phys. Rev. E*, 2019, **99**, 012610.
129 T. Bhattacharjee and S. S. Datta, *Nat. Commun.*, 2019, **10**, 2075.
130 O. Chepizhko and F. Peruani, *Phys. Rev. Lett.*, 2013, **111**, 160604.
131 A. Creppy, E. Clement, C. Douarche, M. V. D'Angelo and H. Auradou, *Phys. Rev. Fluids*, 2019, **4**, 013102.
132 A. Morin, D. Lopes Cardozo, V. Chikkadi and D. Bartolo, *Phys. Rev. E*, 2017, **96**, 042611.
133 R. B. Bird, R. C. Armstrong and O. Hassager, in *Dynamics of polymeric liquids. Vol. Fluids mechanics.* John Wiley and Sons Inc., New York, 1987.
134 J. Sznitman and P. E. Arratia, in *Complex fluids in biological systems*, Springer, 2015, pp. 245-281.
135 G. J. Elfring and E. Lauga, in *Complex fluids in biological systems*, Springer, 2015, pp. 283-317.
136 H. C. Fu, C. W. Wolgemuth and T. R. Powers, *Phys. Fluids*, 2009, **21**, 33102.
137 X. N. Shen and P. E. Arratia, *Phys. Rev. Lett.*, 2011, **106**, 208101.
138 J. Teran, L. Fauci and M. Shelley, *Phys. Rev. Lett.*, 2010, **104**, 038101.
139 B. Liu, T. R. Powers and K. S. Breuer, *Proc. Natl. Acad. Sci. U. S. A.*, 2011, **108**, 19516-19520.
140 S. E. Spagnolie, B. Liu and T. R. Powers, *Phys. Rev. Lett.*, 2013, **111**, 068101.
141 J. Espinosa-Garcia, E. Lauga and R. Zenit, *Phys. Fluids*, 2013, **25**.
142 H. C. Fu, C. W. Wolgemuth and T. R. Powers, *Phys. Rev. E*, 2008, **78**, 041913.
143 E. E. Riley and E. Lauga, *Europhys. Lett.*, 2014, **108**, 34003.
144 B. Thomases and R. D. Guy, *Phys. Rev. Lett.*, 2014, **113**, 098102.
145 D. Salazar, A. M. Roma and H. D. Ceniceros, *Phys. Fluids*, 2016, **28**, 063101.
146 B. Thomases and R. D. Guy, *J. Fluid Mech.*, 2017, **825**, 109-132.
147 T. Normand and E. Lauga, *Phys. Rev. E*, 2008, **78**, 061907.
148 O. S. Pak, T. Normand and E. Lauga, *Phys. Rev. E*, 2010, **81**, 036312.
149 N. C. Keim, M. Garcia and P. E. Arratia, *Phys. Fluids*, 2012, **24**, 081703.

150 O. S. Pak, L. L. Zhu, L. Brandt and E. Lauga, *Phys. Fluids*, 2012, **24**, 103102.
151 C. Datt, B. Nasouri and G. J. Elfring, *Phys. Rev. Fluids*, 2018, **3**, 123301.
152 M. J. Lighthill, *Commun. Pure Appl. Math.*, 1952, **5**, 109-118.
153 J. R. Blake, *J. Fluid Mech.*, 2006, **46**, 199-208.
154 L. Zhu, M. Do-Quang, E. Lauga and L. Brandt, *Phys. Rev. E*, 2011, **83**, 011901.
155 L. L. Zhu, E. Lauga and L. Brandt, *Phys. Fluids*, 2012, **24**, 051902.
156 S. Yazdi, A. M. Ardekani and A. Borhan, *Phys. Rev. E*, 2014, **90**, 043002.
157 S. Yazdi, A. M. Ardekani and A. Borhan, *J. Nonlinear Sci.*, 2015, **25**, 1153-1167.
158 M. De Corato, F. Greco and P. L. Maffettone, *Phys. Rev. E*, 2015, **92**, 053008.
159 T. J. Pedley, *IMA J. Appl. Math.*, 2016, **81**, 488-521.
160 G. Natale, C. Datt, S. G. Hatzikiriakos and G. J. Elfring, *Phys. Fluids*, 2017, **29**, 123102.
161 J. R. Gomez-Solano, A. Blokhuis and C. Bechinger, *Phys. Rev. Lett.*, 2016, **116**, 138301.
162 K. Qi, E. Westphal, G. Gompper and R. G. Winkler, *Phys. Rev. Lett.*, 2020, **124**, 068001.
163 M. R. Shaebani, A. Wysocki, R. G. Winkler, G. Gompper and H. Rieger, *Nat. Rev. Phys.*, 2020, **2**, 181-199.
164 A. Zöttl and J. M. Yeomans, *Nat. Phys.*, 2019, **15**, 554-558.
165 R. Tuinier, J. K. G. Dhont and T. H. Fan, *Europhys. Lett.*, 2006, **75**, 929-935.
166 T. H. Fan, J. K. G. Dhont and R. Tuinier, *Phys. Rev. E*, 2007, **75**, 011803.
167 Y. Man and E. Lauga, *Phys. Rev. E*, 2015, **92**, 023004.
168 A. Kaye, *Nature*, 1963, **197**, 1001-1002.
169 M. Versluis, C. Blom, D. van der Meer, K. van der Weele and D. Lohse, *J. Stat. Mech.: Theory Exp.*, 2006, **2006**, P07007.
170 J. R. Vélez-Cordero and E. Lauga, *J. Non-Newton. Fluid*, 2013, **199**, 37-50.
171 T. D. Montenegro-Johnson, A. A. Smith, D. J. Smith, D. Loghin and J. R. Blake, *Eur. Phys. J. E*, 2012, **35**, 111.
172 T. D. Montenegro-Johnson, D. J. Smith and D. Loghin, *Phys. Fluids*, 2013, **25**, 081903.
173 G. J. Li and A. M. Ardekani, *J. Fluid Mech.*, 2015, **784**, R4.
174 D. A. Gagnon, N. C. Keim and P. E. Arratia, *J. Fluid Mech.*, 2014, **758**, R3.
175 D. A. Gagnon and P. E. Arratia, *J. Fluid Mech.*, 2016, **800**, 753-765.
176 J. S. Park, D. Kim, J. H. Shin and D. A. Weitz, *Soft Matter*, 2016, **12**, 1892-1897.
177 S. Gómez, F. A. Godínez, E. Lauga and R. Zenit, *J. Fluid Mech.*, 2016, **812**, R3.
178 C. Datt, L. L. Zhu, G. J. Elfring and O. S. Pak, *J. Fluid Mech.*, 2015, **784**, R1.
179 E. E. Riley and E. Lauga, *Phys. Rev. E*, 2017, **95**, 062416.
180 K. Pietrzyk, H. Nganguia, C. Datt, L. L. Zhu, G. J. Elfring and O. S. Pak, *J. Non-Newton. Fluid*, 2019, **268**, 101-110.
181 T. Qiu, T. C. Lee, A. G. Mark, K. I. Morozov, R. Munster, O. Mierka, S. Turek, A. M. Leshansky and P. Fischer, *Nat. Commun.*, 2014, **5**, 1-8.
182 K. Han, C. W. t. Shields, B. Bharti, P. E. Arratia and O. D. Velev, *Langmuir*, 2020, DOI: 10.1021/acs.langmuir.9b03698.
183 G. Gheissary and B. H. A. A. vandenBrule, *J. Non-Newton. Fluid*, 1996, **67**, 1-18.
184 Y. J. Liu and D. D. Joseph, *J. Fluid Mech.*, 1993, **255**, 565-595.
185 S. Van Loon, J. Fransaer, C. Clasen and J. Vermant, *J. Rheol.*, 2014, **58**, 237-254.
186 D. D. Joseph and Y. Q. J. Liu, *J. Rheol.*, 1993, **37**, 961-983.
187 M. Dasgupta, B. Liu, H. C. Fu, M. Berhanu, K. S. Breuer, T. R. Powers and A. Kudrolli, *Phys. Rev. E*, 2013, **87**, 013015.
188 A. Beris, R. C. Armstrong and R. A. Brown, *J. Non-Newton. Fluid*, 1983, **13**, 109-148.
189 R. Dong, Y. Hu, Y. Wu, W. Gao, B. Ren, Q. Wang and Y. Cai, *J. Am. Chem. Soc.*, 2017, **139**, 1722-1725.
190 K. M. Manesh, M. Cardona, R. Yuan, M. Clark, D. Kagan, S. Balasubramanian and J. Wang, *ACS Nano*, 2010, **4**, 1799-1804.
191 W. Gao, A. Uygun and J. Wang, *J. Am. Chem. Soc.*, 2012, **134**, 897-900.
192 F. Mou, C. Chen, H. Ma, Y. Yin, Q. Wu and J. Guan, *Angew. Chem. Int. Ed.*, 2013, **52**, 7208-7212.
193 C. Chen, E. Karshalev, J. Guan and J. Wang, *Small*, 2018, **14**, e1704252.
194 W. Gao, X. Feng, A. Pei, Y. Gu, J. Li and J. Wang, *Nanoscale*, 2013, **5**, 4696-4700.
195 J. Li, V. V. Singh, S. Sattayasamitsathit, J. Orozco, K. Kaufmann, R. Dong, W. Gao, B. Jurado-Sanchez, Y. Fedorak and J. Wang, *ACS Nano*, 2014, **8**, 11118-11125.
196 F. Zhang, R. Mundaca-Uribe, H. Gong, B. Esteban-Fernandez de Avila, M. Beltran-Gastelum, E. Karshalev, A. Nourhani, Y. Tong, B. Nguyen, M. Gallot, Y. Zhang, L. Zhang and J. Wang, *Adv. Mater.*, 2019, **31**, e1901828.
197 M. Wan, H. Chen, Q. Wang, Q. Niu, P. Xu, Y. Yu, T. Zhu, C. Mao and J. Shen, *Nat. Commun.*, 2019, **10**, 966.
198 M. M. Stanton, C. Trichet-Paredes and S. Sanchez, *Lab Chip*, 2015, **15**, 1634-1637.
199 F. M. Qiu, S. Fujita, R. Mhanna, L. Zhang, B. R. Simona and B. J. Nelson, *Adv. Funct. Mater.*, 2015, **25**, 1666-1671.
200 M. A. Zeeshan, R. Grisch, E. Pellicer, K. M. Sivaraman, K. E. Peyer, J. Sort, B. Ozkale, M. S. Sakar, B. J. Nelson and S. Pane, *Small*, 2014, **10**, 1284-1288.
201 D. Schamel, A. G. Mark, J. G. Gibbs, C. Miksch, K. I. Morozov, A. M. Leshansky and P. Fischer, *ACS Nano*, 2014, **8**, 8794-8801.
202 L. Ren, N. Nama, J. M. McNeill, F. Soto, Z. Yan, W. Liu, W. Wang, J. Wang and T. E. Mallouk, *Sci. Adv.*, 2019, **5**, eaax3084.
203 F. Soto, A. Martin, S. Ibsen, M. Vaidyanathan, V. Garcia-Gradilla, Y. Levin, A. Escarpa, S. C. Esener and J. Wang, *ACS Nano*, 2016, **10**, 1522-1528.
204 H. Xu, M. Medina-Sanchez, M. F. Maitz, C. Werner and O. G. Schmidt, *ACS Nano*, 2020, **14**, 2982-2993.
205 Y. Alapan, O. Yasa, O. Schauer, J. Giltinan, A. F. Tabak, V. Sourjik and M. Sitti, *Sci. Robot.*, 2018, **3**, eaar4423.
206 S. Chatterjee, *Front Physiol.*, 2018, **9**, 524.
207 N. Korin, M. J. Gounis, A. K. Wakhloo and D. E. Ingber, *JAMA Neurol.*, 2015, **72**, 119-122.
208 T. G. Papaioannou and C. Stefanadis, *Hellenic J. Cardiol.*, 2005, **46**, 9-15.
209 P. L. Venugopalan, R. Sai, Y. Chandorkar, B. Basu, S. Shivashankar and A. Ghosh, *Nano Lett.*, 2014, **14**, 1968-1975.
210 W. Gao, R. H. Fang, S. Thamphiwatana, B. T. Luk, J. Li, P. Angsantikul, Q. Zhang, C. M. Hu and L. Zhang, *Nano Lett.*, 2015, **15**, 1403-1409.
211 C. M. Hu, R. H. Fang, K. C. Wang, B. T. Luk, S. Thamphiwatana, D. Dehaini, P. Nguyen, P. Angsantikul, C. H. Wen, A. V. Kroll, C. Carpenter, M. Ramesh, V. Qu, S. H. Patel, J. Zhu, W. Shi, F. M. Hofman, T. C. Chen, W. Gao, K. Zhang, S. Chien and L. Zhang, *Nature*, 2015, **526**, 118-121.
212 Z. Wu, T. Li, W. Gao, T. Xu, B. Jurado-Sánchez, J. Li, W. Gao, Q. He, L. Zhang and J. Wang, *Adv. Funct. Mater.*, 2015, **25**, 3881-3887.
213 C. M. J. Hu, R. H. Fang, J. Copp, B. T. Luk and L. F. Zhang, *Nat. Nanotechnol.*, 2013, **8**, 336-340.
214 J. Li, P. Angsantikul, W. Liu, B. Esteban-Fernandez de Avila, X. Chang, E. Sandraz, Y. Liang, S. Zhu, Y. Zhang, C. Chen, W. Gao, L. Zhang and J. Wang, *Adv. Mater.*, 2018, **30**, 1704800.

215 Z. Wu, J. Li, B. E. F. de Avila, T. Li, W. Gao, Q. He, L. Zhang and J. Wang, *Adv. Funct. Mater.*, 2015, **25**, 7497-7501.
216 B. Esteban-Fernández de Ávila, P. Angsantikul, D. E. Ramírez-Herrera, F. Soto, H. Teymourian, D. Dehaini, Y. Chen, L. Zhang and J. Wang, *Sci. Robot.*, 2018, **3**, eaat0485.
217 Z. Wu, T. Li, J. Li, W. Gao, T. Xu, C. Christianson, W. Gao, M. Galarnyk, Q. He, L. Zhang and J. Wang, *ACS Nano*, 2014, **8**, 12041-12048.
218 Z. Wu, B. Esteban-Fernandez de Avila, A. Martin, C. Christianson, W. Gao, S. K. Thamphiwatana, A. Escarpa, Q. He, L. Zhang and J. Wang, *Nanoscale*, 2015, **7**, 13680-13686.
219 J. R. Baylis, J. H. Yeon, M. H. Thomson, A. Kazerooni, X. Wang, A. E. St John, E. B. Lim, D. Chien, A. Lee, J. Q. Zhang, J. M. Piret, L. S. Machan, T. F. Burke, N. J. White and C. J. Kastrup, *Sci. Adv.*, 2015, **1**, e1500379.
220 W. Gao, C. M. Hu, R. H. Fang, B. T. Luk, J. Su and L. Zhang, *Adv. Mater.*, 2013, **25**, 3549-3553.
221 O. Lieleg and K. Ribbeck, *Trends Cell Biol.*, 2011, **21**, 543-551.
222 F. Ullrich, C. Bergeles, J. Pokki, O. Ergeneman, S. Erni, G. Chatzipirpiridis, S. Pane, C. Framme and B. J. Nelson, *Invest Ophthalmol. Vis. Sci.*, 2013, **54**, 2853-2863.
223 D. Walker, M. Kübler, K. I. Morozov, P. Fischer and A. M. Leshansky, *Nano Lett.*, 2015, **15**, 4412-4416.
224 F. Peng, Y. Tu, Y. Men, J. C. van Hest and D. A. Wilson, *Adv. Mater.*, 2017, **29**, 1604996.
225 F. Araujo, C. Martins, C. Azevedo and B. Sarmento, *Adv. Drug Deliv. Rev.*, 2018, **124**, 98-106.
226 R. Bansil and B. S. Turner, *Adv. Drug Deliv. Rev.*, 2018, **124**, 3-15.
227 D. Walker, B. T. Kasdorf, H. H. Jeong, O. Lieleg and P. Fischer, *Sci. Adv.*, 2015, **1**, e1500501.
228 B. T. Käsdorf, F. Arends and O. Lieleg, *Biophys. J.*, 2015, **109**, 2171-2181.
229 Z. Wu, J. Troll, H. H. Jeong, Q. Wei, M. Stang, F. Ziemssen, Z. Wang, M. Dong, S. Schnichels, T. Qiu and P. Fischer, *Sci. Adv.*, 2018, **4**, eaat4388.
230 S. Pané, J. Puigmartí-Luis, C. Bergeles, X. Z. Chen, E. Pellicer, J. Sort, V. Počepcová, A. Ferreira and B. J. Nelson, *Adv. Mater. Technol.*, 2019, **4**, 1800575.
231 F. M. Lu and Z. Yuan, *Quant. Imaging Med. Surg.*, 2015, **5**, 433-447.
232 A. R. Kherlopian, T. Song, Q. Duan, M. A. Neimark, M. J. Po, J. K. Gohagan and A. F. Laine, *BMC Syst. Biol.*, 2008, **2**, 74.
233 W. Ke, N. G. Horton, K. Charan and C. Xu, *IEEE J. Sel. Top. Quantum Electron.*, 2014, **20**, 50-60.
234 A. Servant, F. Qiu, M. Mazza, K. Kostarelos and B. J. Nelson, *Adv. Mater.*, 2015, **27**, 2981-2988.
235 Y. B. Zhang, L. Zhang, L. D. Yang, C. I. Vong, K. F. Chan, W. K. K. Wu, T. N. Y. Kwong, N. W. S. Lo, M. Ip, S. H. Wong, J. J. Y. Sung, P. W. Y. Chiu and L. Zhang, *Sci. Adv.*, 2019, **5**, eaau9650.
236 A. Aziz, M. Medina-Sanchez, N. Koukourakis, J. W. Wang, R. Kuschmierz, H. Radner, J. W. Czarske and O. G. Schmidt, *Adv. Funct. Mater.*, 2019, **29**, 1905272.
237 Z. Xu, M. Chen, H. Lee, S. P. Feng, J. Y. Park, S. Lee and J. T. Kim, *ACS Appl. Mater. Interfaces*, 2019, **11**, 15727-15732.
238 D. Vilela, U. Cossío, J. Parmar, A. M. Martínez-Villacorta, V. Gómez-Vallejo, J. Llop and S. Sánchez, *ACS Nano*, 2018, **12**, 1220-1227.
239 J. Yu, D. Jin, K. F. Chan, Q. Wang, K. Yuan and L. Zhang, *Nat. Commun.*, 2019, **10**, 5631.
240 X. H. Yan, Q. Zhou, M. Vincent, Y. Deng, J. F. Yu, J. B. Xu, T. T. Xu, T. Tang, L. M. Bian, Y. X. J. Wang, K. Kostarelos and L. Zhang, *Sci. Robot.*, 2017, **2**, eaaq1155.
241 L. V. Wang and S. Hu, *Science*, 2012, **335**, 1458-1462.
242 A. Aziz, M. Medina-Sanchez, J. Claussen and O. G. Schmidt, *Nano Lett.*, 2019, **19**, 6612-6620.
243 Z. Wu, L. Li, Y. Yang, P. Hu, Y. Li, S. Y. Yang, L. Wang and W. Gao, *Sci. Robot.*, 2019, **4**, eaax0613.
244 M. You, C. Chen, L. Xu, F. Mou and J. Guan, *Acc. Chem. Res.*, 2018, **51**, 3006-3014.
245 B. Dai, J. Wang, Z. Xiong, X. Zhan, W. Dai, C. C. Li, S. P. Feng and J. Tang, *Nat. Nanotechnol.*, 2016, **11**, 1087-1092.
246 J. Zheng, B. Dai, J. Wang, Z. Xiong, Y. Yang, J. Liu, X. Zhan, Z. Wan and J. Tang, *Nat. Commun.*, 2017, **8**, 1438.
247 C. Chen, F. Mou, L. Xu, S. Wang, J. Guan, Z. Feng, Q. Wang, L. Kong, W. Li, J. Wang and Q. Zhang, *Adv. Mater.*, 2017, **29**, 1603374.
248 T. Xu, F. Soto, W. Gao, V. Garcia-Gradilla, J. Li, X. Zhang and J. Wang, *J. Am. Chem. Soc.*, 2014, **136**, 8552-8555.
249 T. Xu, F. Soto, W. Gao, R. Dong, V. Garcia-Gradilla, E. Magaña, X. Zhang and J. Wang, *J. Am. Chem. Soc.*, 2015, **137**, 2163-2166.
250 D. P. Singh, W. E. Uspal, M. N. Popescu, L. G. Wilson and P. Fischer, *Adv. Funct. Mater.*, 2018, **28**, 1706660.
251 F. Mou, J. Zhang, Z. Wu, S. Du, Z. Zhang, L. Xu and J. Guan, *iScience*, 2019, **19**, 415-424.
252 Y. Tu, F. Peng and D. A. Wilson, *Adv. Mater.*, 2017, **29**, 1701970.
253 Q. Wang, R. Dong, C. Wang, S. Xu, D. Chen, Y. Liang, B. Ren, W. Gao and Y. Cai, *ACS Appl. Mater. Interfaces*, 2019, **11**, 6201-6207.
254 F. Peng, Y. Tu, J. C. van Hest and D. A. Wilson, *Angew. Chem. Int. Ed.*, 2015, **54**, 11662-11665.
255 Y. Tu, F. Peng, X. Sui, Y. Men, P. B. White, J. C. M. van Hest and D. A. Wilson, *Nat. Chem.*, 2017, **9**, 480-486.
256 T. Li, X. Chang, Z. Wu, J. Li, G. Shao, X. Deng, J. Qiu, B. Guo, G. Zhang, Q. He, L. Li and J. Wang, *ACS Nano*, 2017, **11**, 9268-9275.
257 J. Toner, Y. Tu and S. Ramaswamy, *Annu. Phys.*, 2005, **318**, 170-244.
258 S. Ramaswamy, *Annu. Rev. Condens. Matter Phys.*, 2010, **1**, 323-345.
259 M. C. Marchetti, J. F. Joanny, S. Ramaswamy, T. B. Liverpool, J. Prost, M. Rao and R. A. Simha, *Rev. Mod. Phys.*, 2013, **85**, 1143-1189.
260 M. J. Shelley, *Annu. Rev. Fluid Mech.*, 2016, **48**, 487-506.
261 D. Saintillan, *Annu. Rev. Fluid Mech.*, 2018, **50**, 563-592.
262 H. Xie, M. M. Sun, X. J. Fan, Z. H. Lin, W. N. Chen, L. Wang, L. X. Dong and Q. He, *Sci. Robot.*, 2019, **4**, eaav8006.
263 J. Yu, B. Wang, X. Du, Q. Wang and L. Zhang, *Nat. Commun.*, 2018, **9**, 3260.
264 J. Zhuang and M. Sitti, *Sci. Rep.*, 2016, **6**, 32135.
265 C. Chen, X. Chang, P. Angsantikul, J. Li, B. Esteban-Fernández de Ávila, E. Karshalev, W. Liu, F. Mou, S. He, R. Castillo, Y. Liang, J. Guan, L. Zhang and J. Wang, *Adv. Biosys.*, 2018, **2**, 1700160.
266 R. Cheng, W. Huang, L. Huang, B. Yang, L. Mao, K. Jin, Q. ZhuGe and Y. Zhao, *ACS Nano*, 2014, **8**, 7746-7754.
267 W. Gao, R. Dong, S. Thamphiwatana, J. Li, W. Gao, L. Zhang and J. Wang, *ACS Nano*, 2015, **9**, 117-123.
268 B. E. de Avila, P. Angsantikul, J. Li, M. Angel Lopez-Ramirez, D. E. Ramirez-Herrera, S. Thamphiwatana, C. Chen, J. Delezuk, R. Samakapiruk, V. Ramez, M. Obonyo, L. Zhang and J. Wang, *Nat. Commun.*, 2017, **8**, 272.
269 J. Li, P. Angsantikul, W. Liu, B. Esteban-Fernandez de Avila, S. Thamphiwatana, M. Xu, E. Sandraz, X. Wang, J. Delezuk, W. Gao, L. Zhang and J. Wang, *Angew. Chem. Int. Ed.*, 2017, **56**, 2156-2161.
270 M. Hoop, A. S. Ribeiro, D. Rösch, P. Weinand, N. Mendes, F. Mushtaq, X.-Z. Chen, Y. Shen, C. F. Pujante, J. Puigmartí-Luis, J. Paredes, B. J. Nelson, A. P. Pêgo and S. Pané, *Adv. Funct. Mater.*, 2018, **28**, 1705920.
271 X. Wei, M. Beltran-Gastelum, E. Karshalev, B. Esteban-

Fernandez de Avila, J. Zhou, D. Ran, P. Angsantikul, R. H. Fang, J. Wang and L. Zhang, *Nano Lett.*, 2019, **19**, 1914-1921.
272 H. Xu, M. Medina-Sanchez, V. Magdanz, L. Schwarz, F. Hebenstreit and O. G. Schmidt, *ACS Nano*, 2018, **12**, 327-337.
273 B. W. Park, J. Zhuang, O. Yasa and M. Sitti, *ACS Nano*, 2017, **11**, 8910-8923.
274 O. Felfoul, M. Mohammadi, S. Taherkhani, D. de Lanauze, Y. Zhong Xu, D. Loghin, S. Essa, S. Jancik, D. Houle, M. Lafleur, L. Gaboury, M. Tabrizian, N. Kaou, M. Atkin, T. Vuong, G. Batist, N. Beauchemin, D. Radzioch and S. Martel, *Nat. Nanotechnol.*, 2016, **11**, 941-947.
275 S. Colabrese, K. Gustavsson, A. Celani and L. Biferale, *Phys. Rev. Lett.*, 2017, **118**, 158004.
276 F. Cichos, K. Gustavsson, B. Mehlig and G. Volpe, *Nat. Mach. Intel.*, 2020, **2**, 94-103.
277 A. C. H. Tsang, E. Demir, Y. Ding and O. S. Pak, *Adv. Intel. Syst.*, 2020, DOI: 10.1002/aisy.201900137.

TOC

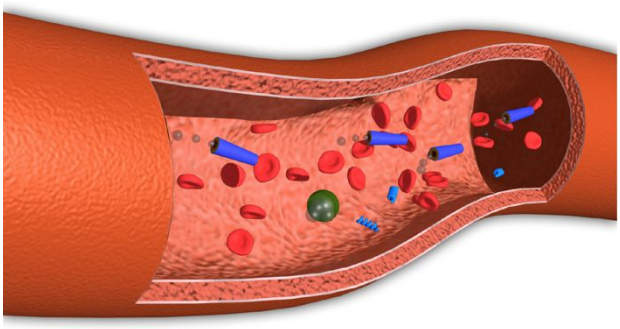

This article introduces how various complex media impact the propulsion of micro/nanorobotics and highlights the emerging technological approaches to enhance the locomotion in complex environments toward practical medical applications *in vivo*.